POLITECNICO
DI TORINO

Facoltà di Ingegneria

Corso di Laurea Magistrale in Ingegneria Aerospaziale

Master Thesis

Low Thrust Manoeuvres To Perform Large Changes of RAAN or Inclination in LEO

Academic Tutor:

Prof. Lorenzo CASALINO

Candidate:

Filippo GRISOT

July 2018

“It is possible for ordinary people

to choose to be extraordinary”

E. Musk

Acknowledgments

I would like to address my sincere acknowledgments to my professor Lorenzo Casalino, for your huge help in these moths, for your willingness, for your professionalism and for your kindness. It was very stimulating, as well as fun, working with you.

I would like to thank all my course-mates, for the time spent together inside and outside the "Poli", for the help in passing the exams, for the fun and the desperation we shared throughout these years. I would like to especially express my gratitude to Emanuele, Gianluca, Giulia, Lorenzo and Fabio who, more than everyone, had to bear with me.

I would like to also thank all my extra-Poli friends, especially Alberto, for your support and the long talks throughout these years, Zach, for being so close although the great distance between us, Bea's family, for all the Sundays and summers spent together, and my soccer team Belfiga FC, for being the crazy lovable people you are.

A huge acknowledgment needs to be address to my family: to my grandfather Luciano, for being a great friend; to my grandmother Bianca, for teaching me what "fighting" means; to my grandparents Beppe and Etta, for protecting me every day from up there; to Becky, Harry and Spyro, for the love you have given me every

single day; to my sister Lulu, for the beautiful moments shared and for those that will be shared in the future; to my sister Gio and her future husband Josè, for the help in inspecting this thesis and all the support from the other side of the ocean; to my mom, for being the beautiful person you are, for teaching me the meaning of willingness and for supporting me in every single moment of my entire life; and to my dad, for being the person and the father I wish to become one day.

Last, but most important, I would like to thank you, Beatrice. You know what for.

Abstract

Space X has proved that space exploration does not belong only to the government anymore, but that private companies can also play an important role in it; this means that, in a future not so far from today, the number of launches will increase exponentially: each company will have its own mission, be it for scientific experiments, Earth observation or interplanetary expeditions. However, they will also need to find the cheapest way to achieve their goals and this study offers a realistic starting point: a long-term orbiting reusable platform. By revisiting a yet outdated NASA project, we developed an optimisation of a transfer between a feasible future space station and one of these platforms, considering a low thrust propulsion. In order to find a solution to reduce time and costs, we analysed how to take advantage of the j_2 orbit perturbation due to the asphericity of Earth. The results of this work offer an accurate overview of the transfer and the values of time and costs for different feasible scenarios.

.

List of Figures

List of Tables

Summary

Chapter 1:

The Project

In this first chapter we would like to present the idea of our study, explaining the reason for it and the interest that a space company may have in it. However, to better understand it, it could be useful, as well as interesting, to first take a look at the history behind. In fact, the idea of this work is to reinvent a yet outdated and interesting old project colliding with the exponential technological progresses achieved throughout these years: it is a reconsideration of an old NASA's purpose, unfortunately abandoned too soon, during the path towards the realisation of the International Space Station (ISS).

In these first paragraphs, we will take an imaginary walk through the story that lead to the ISS focusing, however, on the period of an intermediate evolution of it named "Space Station Freedom". The following paragraphs will give, in the end, a brief overview of the study itself, presenting its goals and the default scenario we considered.

1.1 The Historical Background

1.1.1 The Origin of the Space Race

Already hundred years before the conquest of the Moon by Apollo expeditions, scientists were thinking of and even promising the audience a future with outposts both on the Moon and orbiting the Earth. In the following years, these "outposts" slowly evolved into orbital platforms that could have been the base for future missions to Moon and Mars.

During the last years of the 1860s, the writer Edward Everett Hale captivated the mind of the readers with the chance of living outside the Earth through his science fiction story, *The Brick Moon* [2], and its sequel *Life in the Brick Moon* [3]. Hale tells the story of a 200-foot diameter brick sphere designed to orbit the Earth, wherein characters could not only live, but also communicate with the Earth below.

People started naming these outposts "space stations" only several years later, when German rocket precursor Hermann Oberth, in 1923, conceived a platform launched by massive rockets from Earth and orbiting it, that would had been the starting point for future missions [4]. His idea was shared by Austrian Herman Noordung who, in 1929, envisioned a multiple modules outpost with each modulus serving its own

unique function[5]. Moreover, both in USA and Germany there were scientists, like Robert Goddard, and societies, like the "Verein für Raumschiffahrt" (Society for Space Travel), who were also thinking and starting to develop those "massive rockets" conceived by Oberth. Among the members of the VfR, German Army hired the scientist Wernher von Braun, with the goal of developing liquid rockets for the military.

With the copious financial mean of the Reich before and during World War II, von Braun was able to finally develop a perfectly functioning rocket, the V-2. It is possible to imagine how important this achievement had been for the evolution of the space field, as well as for the War itself. Moreover, with the arrival of the Cold War, USA – where Von Braun moved after the end of the War - and USSR started evolving Von Braun's creature.

Through collaborations with Collier's Magazine and Walt, von Braun brought his vision of a wheel-shaped space station to the public:

"Within the next 10 or 15 years, the Earth will have a new companion in the skies, a man-made satellite that could be either the greatest force of peace ever devised, or one of the most terrible weapons of war – depending on who makes control of it. Inhabited by humans, and visible from the ground as a fast-moving star, it will sweep around the earth at an incredible rate of speed in the dark void beyond the atmosphere which is known as "space". [...] The speed at which the 250-foot-wide "wheel"-shaped satellite will move will be almost [...] 20 times the speed of sound. However, this terrific velocity will not be apparent to its occupants. To them, the space station will appear to be a perfectly steady platform. From this platform, a trip to the moon itself will be just a step, as scientists reckon distance in space*".*

(WERNHER VON BRAUN, *Crossing the last frontier,* Collier's Magazine 22 March 1952)

Men and materials arrive in the winged rocket and take "space taxis" to wheel-shaped space station at right. Men wear pressurized suits

CROSSING THE LAST FRONTIER

By Dr. WERNHER von BRAUN

Technical Director, Army Ordnance Guided Missiles Development Group, Huntsville, Alabama

Scientists and engineers now know how to build a station in space that would circle the earth 1,075 miles up. The job would take 10 years, and cost twice as much as the atom bomb. If we do it, we can not only preserve the peace but we can take a long step toward uniting mankind

Collier's for March 22, 1952

Three "space taxis" can be seen—one leaving rocket, another reaching satellite, a third near the already-built astronomical observatory

WITHIN the next 10 or 15 years, the earth will have a new companion in the skies, a man-made satellite that could be either the greatest force for peace ever devised, or one of the most terrible weapons of war—depending on who makes and controls it. Inhabited by humans, and visible from the ground as a fast-moving star, it will sweep around the earth at an incredible rate of speed in that dark void beyond the atmosphere which is known as "space."

In the opinion of many top experts, this artificial moon—which will be carried into space, piece by piece, by rocket ships—will travel along a celestial route 1,075 miles above the earth, completing a trip around the globe every two hours. Nature will provide the motive power; a neat balance between its speed and the earth's gravitational pull will keep it on course (just as the moon is fixed in its orbit by the same two factors). The speed at which the 250-foot-wide, "wheel"-shaped satellite will move will be an almost unbelievable 4.4 miles per second, or 15,840 miles per hour—20 times the speed of sound. However, this terrific velocity will not be apparent to its occupants. To them, the space station will appear to be a perfectly steady platform.

From this platform, a trip to the moon itself will be just a step, as scientists reckon distance in space.

The choice of the so-called "two-hour" orbit—in preference to a faster one, closer to the earth, or a slower one like the 29-day orbit of the moon—has one major advantage: although far enough up to avoid the hazards of the earth's atmosphere, it is close enough to afford a superb observation post.

Technicians in this space station—using specially designed, powerful telescopes attached to large optical screens, radarscopes and cameras—will keep under constant inspection every ocean, continent, country and city. Even small towns will be clearly visible through optical instruments that will give the watchers in space the same vantage point enjoyed by a man in an observation plane only 5,000 feet off the ground.

Nothing will go unobserved. Within each two-hour period, as the earth revolves inside the satellite's orbit, one twelfth of the globe's territory will pass into the view of the space station's occupants; within each 24-hour period, the entire surface of the earth will have been visible.

Over North America, for example, the space station might pass over the East Coast at, say 10:00 a.m., and, after having completed a full revolution around the earth, would—because the

PAINTING BY CHESLEY BONESTELL

Figure 1: Von Braun's article, Collier's Magazine 22 March 1952

If we take a moment to think about what the ISS is today, it is easy to understand the genius of this man, who was able to plan something fulfilled only 40 years later, in 1998 with the launch of Zarya.

Von Braun's idea had such a great resonance in the scientific and space community that the *National Aeronautic and Space Administration* (NASA) was created to manage all the following spaceflight programs, with the collective goal of getting an astronaut in space before the USSR. NASA was also thinking about a future space station, able to help reaching this goal but, after the success of Vostok I mission, which brought Yuri Gagarin as first into space, NASA had to change its plan and aim at something more than simply taking a man in space: let him walk on the Moon.

Throughout the '60s, NASA focused on Moon landing, but the space station was never truly off the drawing board.

1.1.2 The Space Shuttle and Skylab

Few months before the Apollo 11's launch, NASA proposed a 100-man space station called "Space Base" (Figure 2). It was conceived as an international facility for researches, applications and industry-sponsored microgravity experiments. Moreover, it could serve as support for other space operations such as servicing unmanned satellite to ferry astronauts to the Moon.

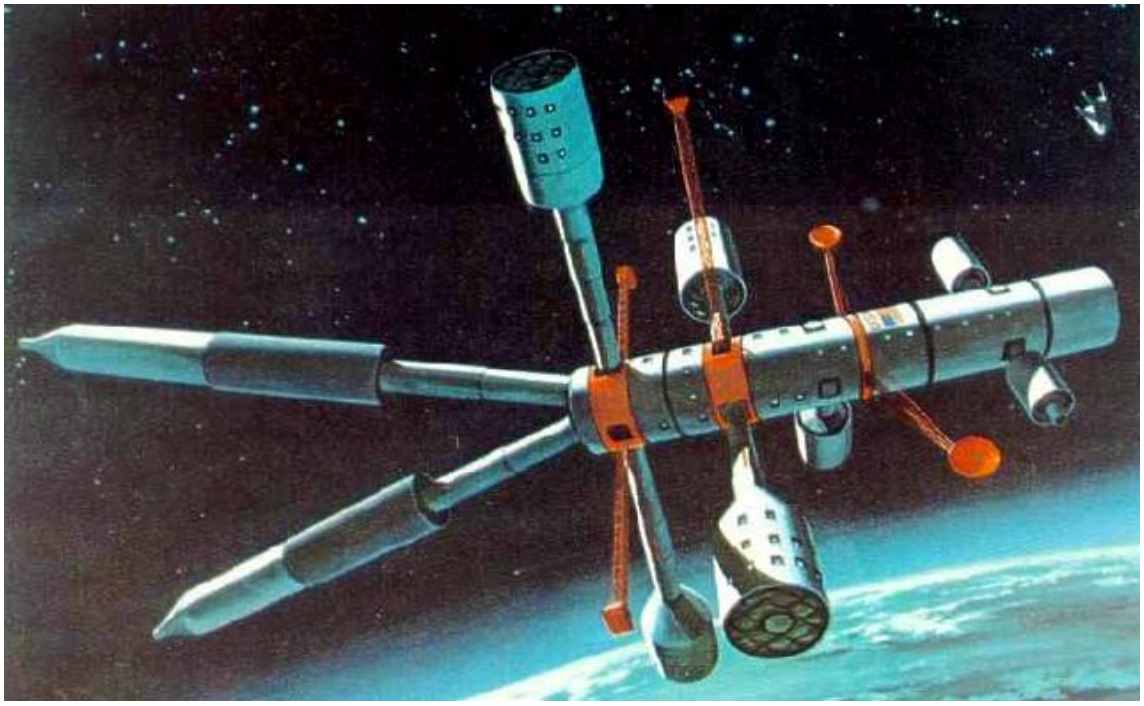

Figure 2: NASA's Space Base [a]

Even though it was scheduled to be completed by 1975, NASA soon realised that the cost of both building and supplying Space Base would exceed the construction cost of the station itself. Therefore, NASA had to plan a cheaper way to achieve the

construction of a space station without changing the concept of it. The main idea was to use a reusable vehicle able to support multiple missions, in order to have a long-term profit from it. This was the birth of the Space Shuttle program [7].

However, since this argument diverts from our study, we will steer our attention to the path towards the ISS. The step that followed "Space Base" was the launch of a short-term space station named "Skylab"[9] (Figure 3).

From its launch on May 14, 1973, until its disposal on July 11, 1979, the Skylab program represented a key proof that humans could live and work in outer space for long periods of time. According to the original plan, the station was supposed to remain in space for more than 15 years, even after the last Skylab mission, becoming not only the greatest solar observatory of its time, but also a laboratory for microgravity and medical experiments, an Earth-observing facility as well as a home for the resident crew. Unfortunately, an intense solar activity forced Skylab to re-enter and disintegrate in Earth's atmosphere much sooner than expected.

Three were the Skylab manned missions, with a crew of three astronauts each. Pete Conrad, Paul Weitz and Joe Kerwin constituted the first crew, which spent 28 days in orbit. The second crew - Alan Bean, Jack Lousma and Owen Garriott - spent 59 days whereas the third - Jerry Carr, Bill Pogue and Edward Gibson - spent 84 days. This final record was broken only a couple of decades later with the Shuttle-Mir program.

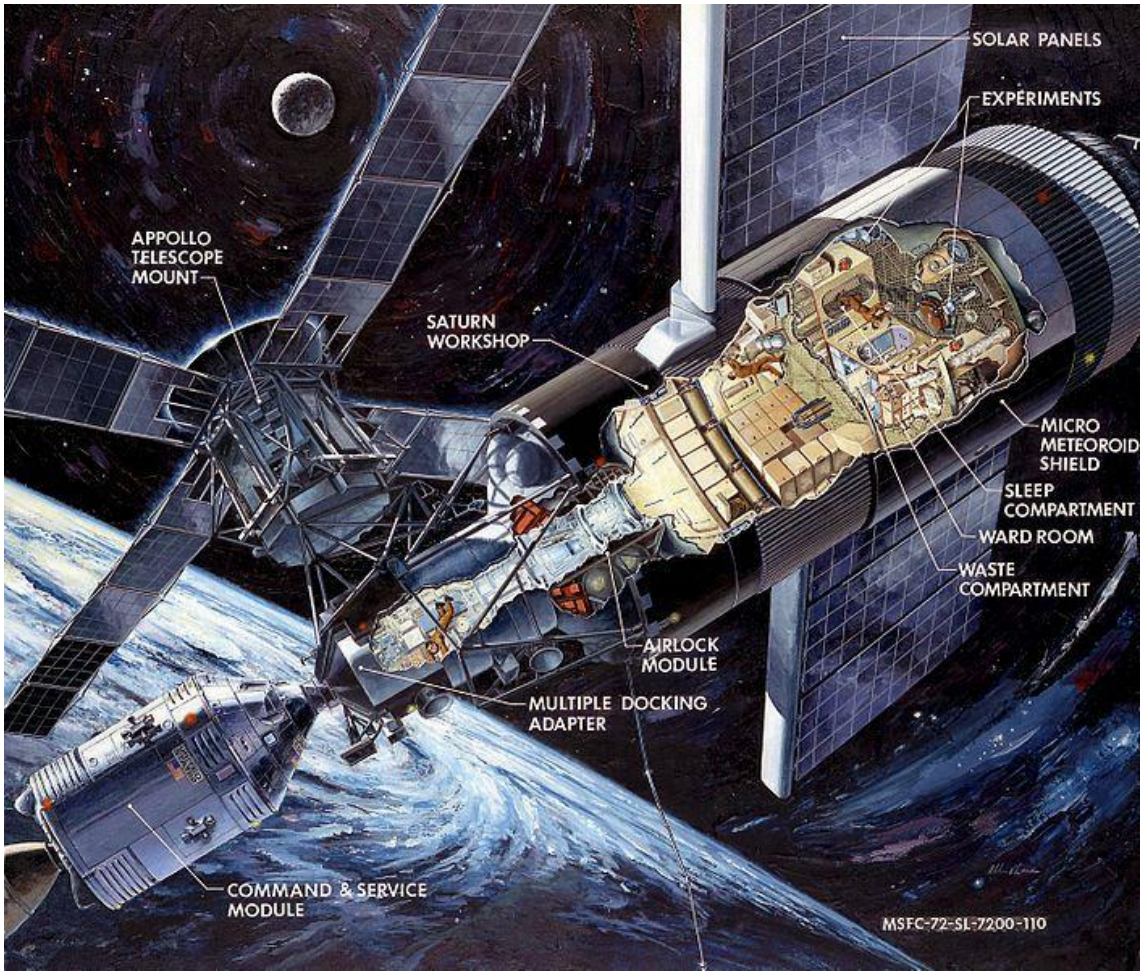

Figure 3: The structure of Skylab [b]

After the short success of Skylab NASA realised that it would have been impossible to economically support a simultaneous building of a reusable space shuttle and of a long-term space station. Therefore, the American space agency was forced to make a choice. And it opted for the shuttle.

1.1.3 A World for… Freedom

After the huge success of the Space Shuttle, NASA started a campaign with the goal of building alliances with international partners, to reduce the costs for the construction of the space station. In 1973, the United States and Europe entered into a partnership wherein the European Space Agency (ESA) had the task to develop mini laboratory modules called Spacelabs. Two years later, Japan and Europe signed on to contribute modules while Canada agreed to supply a manipulator arm. Everything seemed to go exactly the way it was supposed to, but soon new problems surfaced.

Due to an increasing cost – the original estimation was around a third of the effective predicted cost - as well as the Challenger disaster, the original design of a dual keel arrangement with a central truss had to be abandoned and replaced by a single truss design to guarantee more safety. The project was officially finalized in 1987 and American president Reagan gave it the name "Freedom" (Figure 4).

Unfortunately, the Freedom project was soon discarded due to funding complications: the cost of it increased to 38.3 billion dollars, much more than the 8 billions previously forecasted. However, it also represented the foundation for the last and definitive project of a space station that lead to the achievements of the ISS.

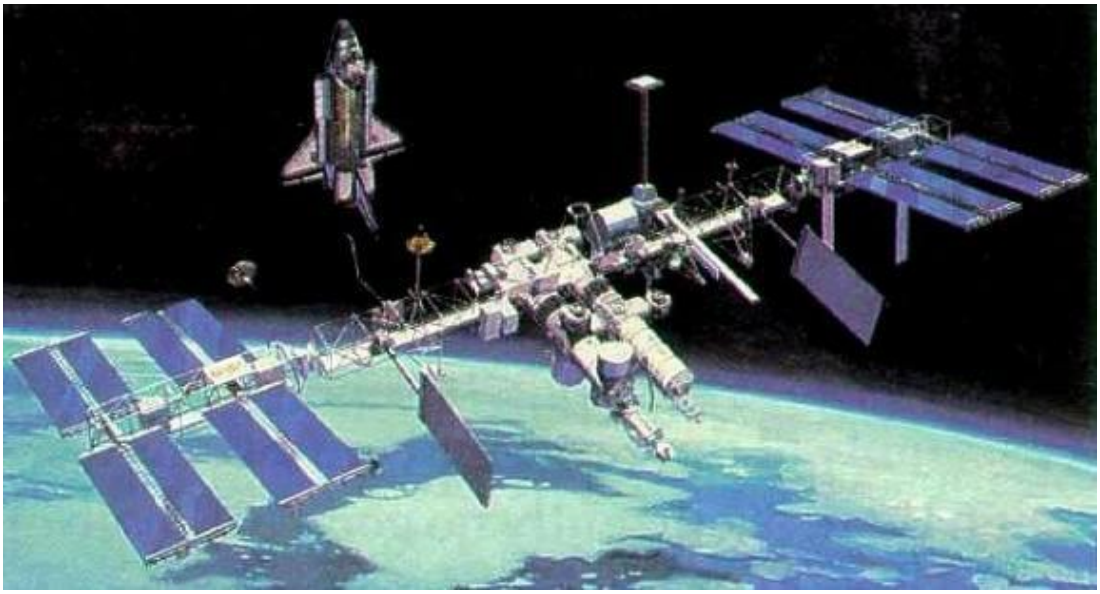

Figure 4: Space Station Freedom [c]

.

The ISS began to take shape in 1998. On November 20th, the Zarya Control Module was launched. It was the first piece of the station onto which later modules were added. On October 30th 2000, NASA launched, on a Soyuz rocket, the crew composed of Yuri P. Gidzenko, William M. Shepherd, and Sergei K. Krikalev, who became the first to live and work on board the orbiting outpost. Another 32 assembly missions had to be accomplished before the completion of the ISS, bringing the dream of a space station to life more than a century after Hale's imagination.

1.2 The Orbital Manoeuvre Vehicle

Around a decade before Freedom was developed and while the Space Shuttle project, excessive solar activity and, consequently, cumulative drag, caused NASA's Skylab to suffer an early deorbit schedule, on July 11th, 1979. Therefore, many contingencies were explored in the last days of its orbital life to try to somehow reboost it and postpone its disposal. One of these solutions consisted in grabbing Skylab and dragging it to a safe orbit with a system named *Teleoperator Retrieval System* (TRS) [10].

No solution was found in time to save Skylab, but NASA decided to keep conducting advanced studies on what was then called *Space Tug*, i.e. a spacecraft (S/C) capable of transferring objects, such as satellites, payloads or debris, from an orbit to another. However, NASA had to temporarily suspend its development in order to focus entirely on the Space Shuttle program. Once the Shuttle was operative, NASA got back again on Space Tug projects, renaming it Orbital Manoeuvring Vehicle (OMV) (Figure 5) [11] [12] [13].

Figure 5: The Orbital Manoeuvring Vehicle

The OMV was meant to be a reusable, remotely controlled, free-flying vehicle and able to perform a wide range of on-orbit missions and services in support of orbiting spacecrafts. It should have represented an important extension of the Space Transportation System (STS), capable of operating from the Shuttle, the Space Station (Freedom at that time), or simply being space based.

The project consisted of a 5m - diameter spacecraft, equipped with reaction control system, avionics systems for electrical power, communications, data management, guidance, navigation, and a 6-degree of freedom control. The estimation of its weight was around 3000 Kg. The OMV was planned to be powered with primary batteries as well as by solar array panels to face potential long-term missions. NASA also designed to locate all critical avionics components in accessible locations to permit an on-orbit maintenance and repair capability.

It is easy to understand the benefits offered by OMV: it was capable of retrieving a spacecraft to the Shuttle or to Freedom and then redeploy it to its operational altitude after the maintenance; it could operate refuelling and hardware replacement to on orbit assets and also serve as a payload support platform. No orbital refuelling of the OMV was assumed, since it could contain enough fuel to get back itself to the departure base at the end of the mission.

The OMV development program started in 1986 and its designed lifetime was of 10 years, with over 40 launches/landings. However, even though the first flight was scheduled on 1991, it never took place because the program was cancelled at the beginning of '90s.

1.3 European Retrievable Carrier

EURECA (European Retrievable Carrier)[15][17][f] was a free-flying retrievable carrier of experiments which was launched and recovered by the Space Shuttle. It was developed by *Deutsche Aerospace* (DASA) on behalf of ESA as a re-usable, multi-disciplinary platform for microgravity, science and technology missions. EURECA development began in 1984: the initial plan considered 5 missions of an approximately 6 - 9 months duration each and an on-ground turn-around time of maximum two years.

Its first mission started on July 31st, 1992 when EURECA left Cape Canaveral launch base as part of the payload in the Space Shuttle Atlantis cargo bay. Atlantis deployed EURECA on August 2nd using the Remote Manipulator System (RMS) and the satellite raised its orbit to the final altitude of 508 Km. The entire mission was monitored from the ESA Mission Control Centre in Darmstadt (Germany) throughout all phases, but some payload operations were provided also by the Microgravity User Support Centre of the *Deutsches Zentrum für Luft- und Raumfahrt* (DLR) in Cologne (Germany). The payload included 16 active instruments: six for microgravity research, two for space radiation research, five for space science research and three for technology demonstrations.

Although great importance was given to its abundant and continuous data generation, two were the primary objectives of EURECA mission:

1) the post-flight analysis, in ground-based laboratories, of biological and material samples collected during the mission;
2) the ability of the spacecraft and its payloads to be ready for a new flight in a quite limited lapse of time.

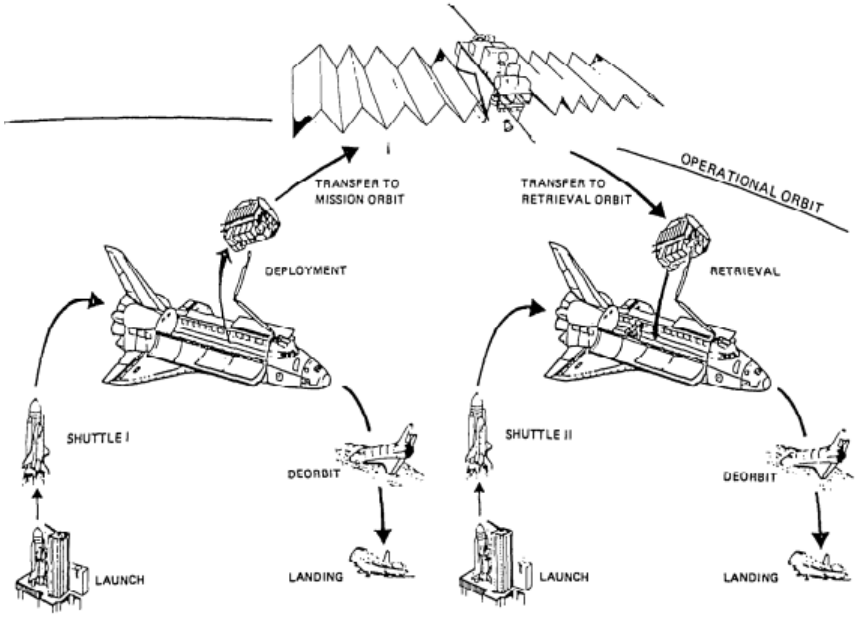

Figure 6: EURECA's Flight Scenario [g]

EURECA started its disposal operations around the half of May 1993, about a month before the lift-off of the Shuttle Endeavour, designated to bring EURECA back home. EURECA descended to a parking orbit of 474 Km and then waited three days before the rendezvous with the Shuttle. Endeavour's crew completed the retrieval mission, grabbing EURECA with the RMS and stowing it in the cargo bay. Endeavour's landing took place on July 1st, 1993.

Bringing EURECA back to Earth proved to be an invaluable contribution not only to payload and mission product owners, but also to technical companies dealing with in-orbit performance validation and, in particular, with the identification of the causes of in-orbit anomalies. Results of spacecraft in-flight anomalies investigations often point to several potential sources of failure which can be sufficient for workaround mission continuation but are unable to reveal the real causes; only post flight on-ground investigations provide this information. Results of this nature from the first EURECA flight have provided important contributions for the improvement of following satellites.

Although EURECA would have been a valid low-cost option as on orbit multiple experiments platform, the project was abandoned by NASA after the first flight to fully concentrate on the realisation of the ISS.

We have revisited this idea, trying to give a modern interpretation of it.

1.4 The Scenario

We would like to first show the scenario we considered, which also represents the simplest one, aware that any other scenario might be easily created from ours. We will then present a brief overview of our study, which will be fully deepen in the following chapters.

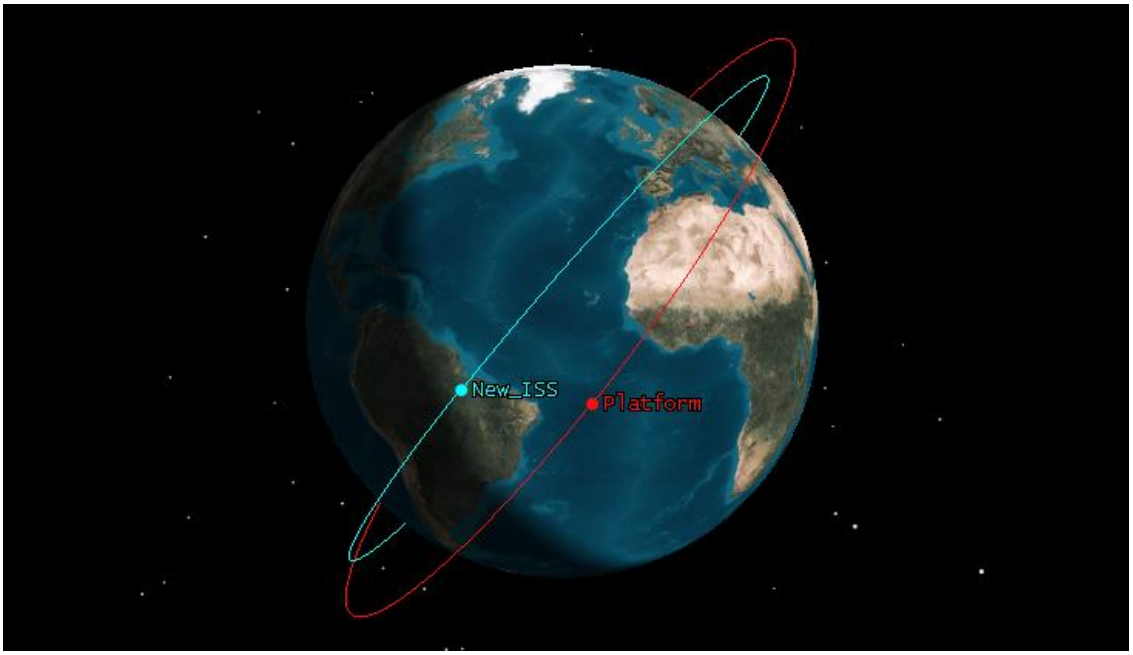

Figure 7: The Scenario

As already mentioned, the scenario of our study is very simple and consists of two elements (Figure 7):

- "New_ISS" is a new concept for the ISS; this study needs, indeed, to look beyond the forthcoming future, considering a disposal of the current ISS and a following feasible new similar outpost positioned on an orbit not so different from the previous one;

- "Platform" represents one of the orbiting long-term reusable platform presented in the abstract.

The two satellites present the same inclination of 51.6° - the one of the current ISS – but different altitude and Right Ascension of the Ascending Node (RAAN).

> RAAN is the angle from the origin of longitude of the reference plane (directed towards Aries constellation) to the orbit's ascending node which is the point where the orbiting body crosses the reference plane, while going "upward". Considering the 2D vision of the ground track, the RAAN shifts the ground track left and right.

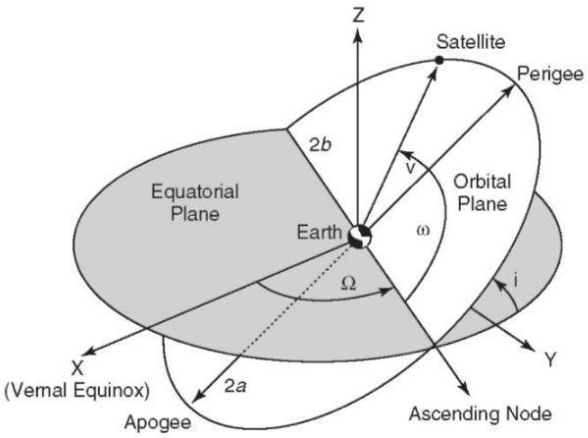

Figure 8: Orbital Angles [i]

New_ISS has an altitude of 500 km (very similar to the current one) whereas the platform is positioned above of it, but the altitude is not given because different values of it will be considered. The same happens with the RAAN difference.

For the transfer, a low-thrust propulsion is considered.

We have set some default parameters for the transfer (S/C), to be able to give effective numerical results:

- Since we are considering low-thrust propulsion, we used a specific impulse (I_{sp}) of $2500\ s$, which represents a mean value amongst those available nowadays.
- The thrust value is $0.01\ N$.
- The mass of the S/C is $15\ Kg$

All these values may affect the final results with different intensity: although this problem diverts from the goal of this work, in Chapter 3 we decided to give an overview of the influence of each parameter on the final results so that a feasible interested space company may have a more accurate prediction of the interested case.

1.5 The Study at a Glance

We would like to summarise in these few lines the study we have conducted throughout these months.

Our goal was to optimise the transfer between two orbits with same inclination but different RAAN, considering a low thrust manoeuvre. Key objective of the work was to include in the optimisation the perturbation j_2, which will be briefly presented in the next chapter. It has a really important role in this study, since it is possible to use it to save fuel and time simultaneously.

The first step was to analytically obtain an optimisation of Edelbaum equations (introducing the contribution of j_2) through the Optimisation Control Theory (OCT) discussed in the next chapter; then, we compiled a MATLAB code to perform the integration of the OCT differential equations using a Genetic Algorithm to converge to the global optimum; finally, we generated various graphs to summarize the results of the study and probed different scenarios to offer a broader overview of the results themselves.

1.6 References

1.6.1 Bibliography

1. AMY SHIRA TEITEL, *A Brief History of Space Stations before the ISS, Popular Science, 23 November 2015*
2. HALE E.E., *The Brick Moon*, Atlantic Monthly, 1869
3. HALE E.E., *Life in the Brick Moon*, Atlantic Monthly, 1870
4. OBERTH H., *The Rocket into Planetary Space*, De Gruyter, 1923
5. NOORDUNG H*., "Das Problem der Befahrung des Weltraums",* der Raketen-Motor 1929
6. VON BRAUN W., *Crossing the Last Frontier*, Collier's Magazine, 1952
7. HEPPENHEIMER T.A., "*Space Shuttle Decision",* NASA Tech Report 1947
8. NASA Technology Report*, Space Station Freedom User's Guide, 1992*
9. M. WILLIAMS, History of the NASA Skylab, America's first space station, Universe today June 2015
10. O'DONNEL B., DUNCAN C., *NASA develops teleoperator retrieval system,* NASA FactSheet, 1978
11. PEPPER R. C., *OMV Payload Support Concept for Pegasus Boosted Payloads*, September 1989
12. HUBER W. G., *Orbital maneuvering vehicle: A new capability,* Acta Astronautica 1988

13. HUBER W. G., CRAMBLIT D. C, *Orbital Maneuvering Vehicle (OMV) Mission Applications and System Requirements,* (April 1, 1984). The Space Congress Proceedings. Paper 6

14. HUGH L. MCMANUS, TODD E. SCHUMAN, *Understanding the orbital transfer vehicle trade space,* American Institute of Aeronautics and Astronautics, 2003

15. DOVER A., ACETI R., DROLSHAGEN G., *EURECA 11 months in orbit,* NASA Tech Report

16. WIMMER W., *Eureca Re-Flights: Opportunities for Very-Low-Cost and Cost-Efficient Space Missions*

17. R. MORY, G. SEIBERT, *Eureca: an evolutionary space carrier for microgravity, earth observation and technology demonstration,* NASA Tech Report

1.6.2 Sitography

a) *www.astronautix.com/s/spacebase*

b) *www.nasa.gov/missions/shuttle/f_skylab1*

c) *www.astronautix.com/s/spacestationfreedom*

d) *en.wikipedia.org/wiki/Space_Station_Freedom*

e) *www.space.com/19359-freedom-space-station-concept*

f) *heasarc.gsfc.nasa.gov/docs/heasarc/missions/EURECA*

g) *directory.eoportal.org/web/eoportal/satellite-missions/e/EURECA*

h) *en.wikipedia.org/wiki/European_Retrievable_Carrier*

i) *www.mat.uniroma2.it/celletti/Celletti_OrbitalDeterminatio*

Chapter 2:

The Theory Behind

In this chapter we would like to present the basis of our study: everything the reader needs to know to better understand the presented work. We will take stock of most of the theoretical steps we walked through in these months that allowed us to reach the results presented in the next chapter.

First, we will present the equations of motion, called Lagrange's Equations or Planetary Equations[1] [2], which represent the cornerstone of our work and the point where it all began; then, a brief overview of the perturbation j_2 [2] [5] will be given in order to understand the reason of our keen interest of it; at a later time, the Optimisation Control Theory (OCT) will be presented[6] [7] [8], used to perform the optimisation of the equations, considering the perturbation j_2; finally, we will tackle the Boundary Value Problem (BVP)[c] [d] and explain one possible method to solve it, the Genetic Algorithm[13] .

2.1 Planetary Equations of Motion

In 1808 the Italian mathematician Giuseppe Lodovico Lagrangia, better known as Joseph-Louis Lagrange, performed the theory of variation of parameters, which still represents one of the most important methods for computation of perturbed orbits. The cornerstone of this theory is the concept of *osculating orbit*, which is the gravitational Kepler orbit (i.e. ellipse or other conic) that the S/C would have if perturbations were not present. Hence, it is the orbit that coincides with the current orbital state vectors $\vec{r}$ (position) and $\vec{V}$ (velocity).

The concept of osculating orbit can be remarkably useful: any variation of the osculating elements may be written referred to the perturbating forces and this allows to better physically understand the significance of their effects on the orbit. Orbital Keplerian parameters (Semimajor axis a, Inclination i, Eccentricity e, Argument of periapsis ω and RAAN Ω) are constant for Keplerian orbit and can be uniquely determined by the position $\vec{r}$ and the velocity $\vec{V}$.

Lagrange Equations (Edelbaum equations[3] are a particular type of them) are first-order differential equations, expressing the Keplerian elements variations, due to perturbing forces, with respect to time. There are many versions of them, since they can be rewritten in many ways depending on the study itself and on the reference

system. These equations do not have any analytical solution but rather it is necessary to resort to numerical algorithms or to analytical approximating techniques. This is possible due to the fact that orbital elements are constant for a Keplerian orbit.

We will first see the general formulation and then the one rewritten referring to our study.

$$
\begin{aligned}
\frac{da}{dt} &= -\frac{\partial \tilde{R}}{\partial \tau}\frac{2a^2}{\mu} \\
\frac{de}{dt} &= -\frac{a(1-e^2)}{\mu e}\frac{\partial \tilde{R}}{\partial \tau} - \frac{1}{e}\sqrt{\frac{1-e^2}{\mu a}}\frac{\partial \tilde{R}}{\partial \omega} \\
\frac{di}{dt} &= \frac{1}{\sqrt{\mu a(1-e^2)}\sin i}\left(\cos i\frac{\partial \tilde{R}}{\partial \omega} - \frac{\partial \tilde{R}}{\partial \Omega}\right) \\
\frac{d\omega}{dt} &= \sqrt{\frac{1-e^2}{\mu a}}\left(\frac{1}{e}\frac{\partial \tilde{R}}{\partial e} - \frac{\cot i}{1-e^2}\frac{\partial \tilde{R}}{\partial i}\right) \\
\frac{d\Omega}{dt} &= \frac{1}{\sqrt{\mu a(1-e^2)}\,\sin i}\frac{\partial \tilde{R}}{\partial i} \\
\frac{d\tau}{dt} &= \frac{\partial \tilde{R}}{\partial a}\frac{2a^2}{\mu} + \frac{a(1-e^2)}{\mu e}\frac{\partial \tilde{R}}{\partial e}
\end{aligned}
\tag{2.1}
$$

General formulation of the Lagrange's Planetary Equations

where:

$a = Semimajor\ axis$

$e = Eccentrity$

$t = Time$

$\omega = Argument\ of\ Periapsis$

$\tau = Time\ at\ which\ the\ body\ is\ at\ the\ pericenter$

$i = Inclination$

$\mu = Gravitational\ constant$

$\Omega = RAAN$

Particular attention should be paid to $\tilde{R}$, which represents the disturbing function. This parameter is introduced to simplify the equations since, if every perturbing forces are expressible through a potential, the equation of motion of a satellite can be written in the form

$$\frac{d^2r}{dt^2} + \frac{\mu}{r^3}\hat{r} = \nabla\tilde{R} \tag{2.2}$$

Some observations might be done looking at this first formulation (Eq. 2.1):

- The variation of the semimajor axis is the only one that does not present dependency on any other Keplerian parameters except for τ; it depends only on the initial semimajor axis and the perturbing forces;
- Eccentricity is accountable for the variation of the other parameters, except for the Semimajor axis;
- Variation of i and Ω are very similar, which will be even more clear in the next formulation.

As previously mentioned, Eq. 2.1 represent the planetary equations in terms of the classical Keplerian elements. However, a Keplerian orbit can be described as a function of any other six independent parameters, combination of the classical elements. Therefore, it may be useful for us to consider these six different parameters:

$$\begin{aligned} \alpha_1 &= -\mu/2a & \beta_1 &= -\tau \\ \alpha_2 &= \sqrt{\mu a(1-e^2)} & \beta_2 &= \omega \\ \alpha_3 &= \sqrt{\mu a(1-e^2)}\cos i & \beta_3 &= \Omega \end{aligned} \tag{2.3}$$

One can easily notice that α_1 represents the total energy, while α_2 and α_3 the angular momentum and its component about the z-axis, respectively.

With this set of parameters, Lagrange's equations become very simple:

$$\begin{aligned} \frac{d\alpha_1}{dt} &= \frac{d\tilde{R}}{d\beta_1} \quad , \quad \frac{d\beta_1}{dt} = -\frac{d\tilde{R}}{d\alpha_1} \\ \frac{d\alpha_2}{dt} &= \frac{d\tilde{R}}{d\beta_2} \quad , \quad \frac{d\beta_2}{dt} = -\frac{d\tilde{R}}{d\alpha_2} \\ \frac{d\alpha_3}{dt} &= \frac{d\tilde{R}}{d\beta_3} \quad , \quad \frac{d\beta_3}{dt} = -\frac{d\tilde{R}}{d\alpha_3} \end{aligned} \tag{2.4}$$

This particular form of the equations is named "canonical" and the perturbing potential is called "perturbed Hamiltonian". In deriving the planetary equations, it may be useful to consider that:

$$\frac{d\tilde{R}}{d\alpha_i} = a_x \frac{\partial x}{\partial \alpha_i} + a_y \frac{\partial y}{\partial \alpha_i} + a_z \frac{\partial z}{\partial \alpha_i} \tag{2.5}$$

where a_x, a_y, a_z are the components of the perturbing acceleration along the respective axis. Since partial derivatives are easy to determine, the equations can be written in terms of the perturbing acceleration; thus, we can define these acceleration components as follows:

$$\boldsymbol{A_u = A\, sin\alpha \cos\beta}$$

$$component\ in\ the\ orbital\ plane\ and\ perpendicular\ to\ the\ velocity\ vector$$

$$\boldsymbol{A_v = A\, cos\alpha \cos\beta}$$

$$component\ along\ the\ velocity\ vector$$

$$\boldsymbol{A_w = A \sin\beta}$$

$$component\ out\ of\ the\ orbit\ plane\ in\ the\ direction\ of\ the\ orbital\ momentum$$

It is now possible to rewrite the last formulation of the planetary equations, setting the stage for the next chapter. This formulation has been written assuming small eccentricity (semi-circular orbits) and small inclination.

$$\frac{da}{dt} = \frac{2aA_v}{V_0}$$

$$\frac{de}{dt} = \frac{2\cos\nu\, A_v + \sin\nu\, A_u}{V_0}$$

$$\frac{di}{dt} = \frac{\cos(\omega+\nu)\, A_w}{V_0} \qquad (2.6)$$

$$\frac{d\Omega}{dt} = \frac{\sin(\omega+\nu)\, A_w}{iV_0}$$

$$\frac{d\omega}{dt} = \frac{\frac{2\sin\nu\, A_v}{e} + \frac{\cos\nu\, A_u}{e} - \frac{\sin(\omega+\nu)\, A_w}{i}}{V_0}$$

- *V_0 is the orbital velocity;*
- *ν is the true anomaly.*

Edelbaum Planetary Equations

2.2 Orbital Perturbations

As we already described, different forces act on the orbiting satellite and these forces are responsible for the variation of the classical elements we mentioned about in the previous paragraph. These forces, however, are considerably less intense compared to the gravitational one; for this reason, they are, usually, neglected, especially with high-thrust transfers. In our case, instead, the transfer lasts for a longer lapse of time, long enough to make these effects significant (here one can better understand the difference between the real orbit, i.e. perturbed, and the osculating one).

Orbital perturbation[a] [b] can be classified in terms of their effect on classical elements:

- Secular variations represent a linear variation in the elements;
- Long-term (or -period) variations are periodic perturbations, having a period greater than the orbital period;
- Short-term (or -period) are those with a shorter period than the orbital one.

We will focus on the first group because they represent those that are, usually, neglectable.

2.2.1 Third-Body Perturbation

The first perturbation is named *Third-body perturbation* and represents the effect of the combination of Sun and Moon's gravitational forces. This disturbance causes periodic variations in all the orbital elements, but only three of them are subject to secular variations and only two have relevant consequences on the spacecraft orbit: the variation of the longitude of the ascending node Ω and the argument of perigee ω. The higher is the orbit, the more intense is the effect. For quasi-circular orbits, these variations can be expressed as:

$$Longitude\ of\ the\ ascending\ node \begin{cases} \Omega_{moon} = -\dfrac{0.00338\cos(i)}{n} \\ \Omega_{sun} = -\dfrac{0.00154\cos(i)}{n} \end{cases}$$

$$Argument\ of\ Perigee \begin{cases} \omega_{moon} = \dfrac{0.00169(4 - 5\sin^2(i))}{n} \\ \omega_{sun} = \dfrac{0.00077(4 - 5\sin^2(i))}{n} \end{cases} \tag{2.7}$$

where i is the orbit inclination, n is the number of orbit revolutions per day, while Ω and ω are in degrees per day.

2.2.2 Atmospheric Drag

The second perturbation is due to the atmospheric drag. This effect is clearly more intense closer to Earth and this is usually used for deorbiting and disposal operations at the end of S/C's life. The drag force D on a body acts in the opposite direction of the velocity vector and is given by the equation

$$D = \frac{1}{2} S C_D \rho V^2 \tag{2.8}$$

where C_D is the drag coefficient, ρ is the air density, V is the body's velocity, and S is the area of the body normal to the flow.

Solar activity has also a relevant effect on atmospheric density, which arises with high solar activity. Although solar activity has a slight effect when proximal to Earth, at satellite altitudes the density variations between solar maximum and solar minimum are very important; a consequence of this is that satellites decay more rapidly during periods of solar maxima and much slower during solar minima.

For quasi-circular orbits we can approximate the changes in Semimajor axis, period, and velocity per revolution using the following equations:

$$\Delta a_{rev} = \frac{-2\pi C_D S \rho a^2}{m}$$

$$\Delta T_{rev} = \frac{-6\pi^2 C_D S \rho a^2}{mV} \tag{2.9}$$

$$\Delta V_{rev} = \frac{\pi C_D S \rho a V}{m}$$

2.2.3 Solar Radiation Pressure

Third perturbation is due to *Solar Radiation Pressure* (SRP) which causes variation in all of the orbital elements. The intensity of this effect (acceleration) can be quantified through this equation:

$$a_R = -\frac{4.5 \cdot 10^{-8}\, S}{m} \tag{2.10}$$

For low orbit, atmospheric drag results greater than solar radiation acceleration, for high orbit occurs the opposite.

2.2.4 Asphericity of the Earth

The last perturbation [16] [2] [5] explained in this chapter is the one that most we are interested in. Generally, we assume that Earth is a perfect sphere, especially when writing the 2-body equations of motion; however, it is well known that Earth has a particular shape named *Geoid* which is oblate. This oblateness is responsible for this perturbation: the excess of mass at the equators generates a slight torque on the satellite about the centre of the Earth, which causes the line of nodes (and consequently the orbital plane) to move eastward for retrograde orbits and westward for direct ones.

To derive the equation that we will use in the optimisation to add the j_2 effect, it is necessary to define the gravitational potential of the Earth, expressed in the geocentrical equatorial frame:

$$\varepsilon_g = -\frac{\mu}{r}\left\{1 - \sum_{n=2}^{\infty} j_n \left(\frac{R_E}{r}\right)^n P_n(\sin Lat) - \right. \\ \left. + \sum_{n=2}^{\infty}\sum_{m=1}^{n} j_{n,m}\left(\frac{R_e}{r}\right)^n P_n^m(\sin Lat)\cos\left(Lon - Lon_{n,m}\right)\right\} \tag{2.11}$$

R (position), Lat (latitude) e Lon (longitude) are the spherical coordinates of the S/C in the reference system. P_n represents the n-degree Legendre Polynomial, expressed by Eq. 2.12 while P_n^m is the associated Legendre function of degree n and order m as defined by Eq. 2.13

$$P_n(x) = \frac{1}{2^n n!}\frac{d^n}{dx^n}[(x^2-1)] \tag{2.12}$$

$$P_n^m(x) = (-1)^m(1-x^2)^{\frac{m}{2}}\frac{d^m}{dx^m}[P_n(x)] \tag{2.13}$$

j_n , $j_{n,m}$ and $Lon_{n,m}$ are numerical coefficients and particular attention should be given to the first two. $j_{n,m}$ are called *tesseral* (if $n \neq m$) and *sectorial* (if $n = m$) *harmonics* and are responsible for the deviation in the East-West direction. This effect is, however, generally considered unimportant since it is cancelled by the rotation of the Earth with respect to S/C frame, with exception of GEO satellites, where Earth seems fixed and this effect is very important.

Zonal harmonics j_n describe the North-South deviation and are all in the order of 10^{-6}, except the second, j_2, which is three orders of magnitude greater and has a value of $1.082639 \cdot 10^{-3}$: this is why its effect is definitely less neglectable than the others'.

Although in the general perturbation method three orbital elements are affected by the variation of j_2 (ω , Ω and τ), the only effect we are interested in is described by:

$$\frac{d\Omega}{du} = -3\mu j_2 R_E^2 \frac{\cos i \, sin^2 \, u}{r^3 \sqrt{\mu p}} \frac{dt}{du} \tag{2.14}$$

where $u = \omega + \nu$ and p is the semi latus rectum.

Knowing that

$$\frac{du}{dt} = \frac{\sqrt{\mu p_0}}{r_0^2} \tag{2.15}$$

where the index "0" refers to unperturbed conditions, it is possible to easily obtain the variation in time of the Right Ascension of the Ascending Node which will be used in the optimisation in the next chapters.

We have characterised j_2 perturbation analytically, but it may also be useful to understand it physically, in order to help those less space-familiar readers to appreciate the great interest we have in it. For this reason, we would like to compare the scenario shown in Chapter 1 (Figure 7) and the situation of the same scenario one and two months later (Figures 9 and 10).

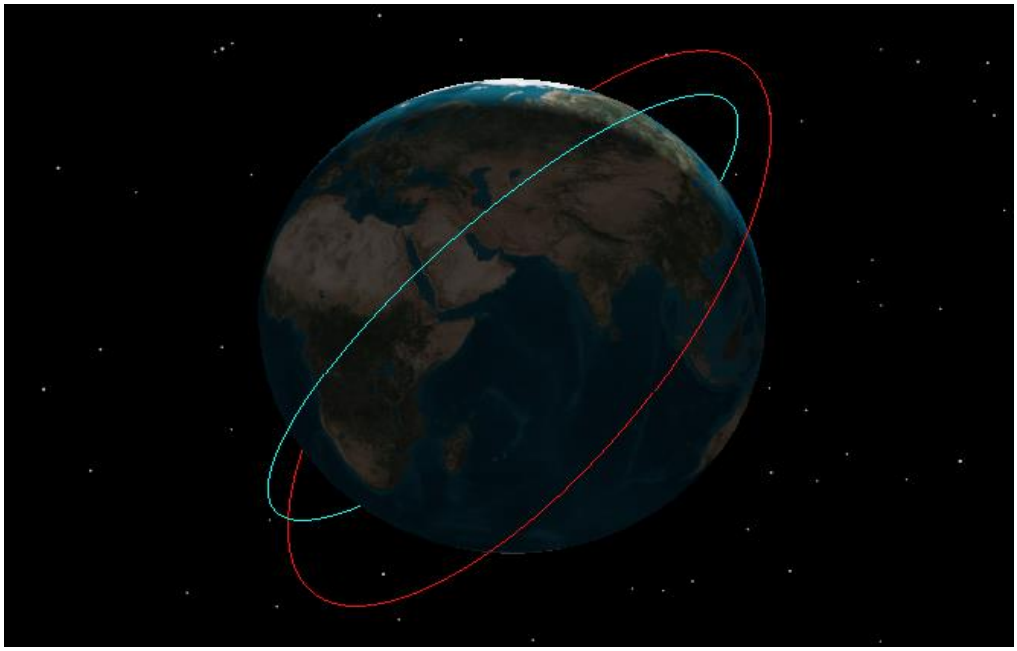

Figure 9: The scenario after 1 month

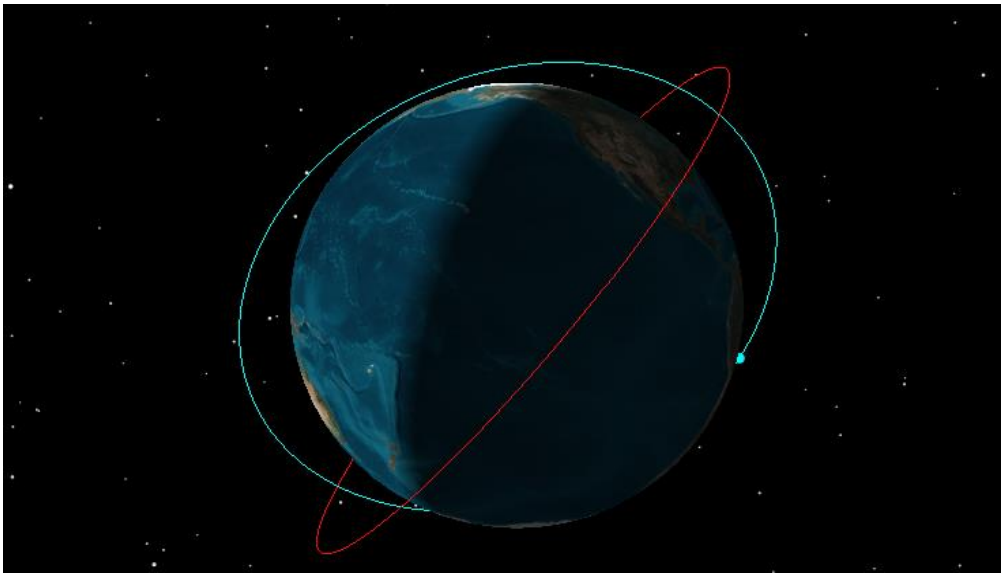

Figure 10: The scenario after 2 months

j_2 perturbation causes a rotation of the orbit plane and, as we said, the lower is the orbit, the greater is the effect. Considering two orbital planes with different heights, there will be a mutual rotation of them, which means that there will be a certain moment in which the two planes will coincide. It is easy to understand that the smaller is the mutual angle between the two orbital planes, the cheaper will be the transfer between them (since Hohmann coplanar transfer is the cheapest transfer possible). Therefore, the goal of this work is to study how to take advantage of this effect to reduce the RAAN difference and consequently time and costs of the manoeuvre between the two orbits.

2.3 Optimal Control Theory

Throughout the last 100 years, one of the biggest problem space scientists have faced, has been the very high cost of a space mission, even the simplest "imaginable". Therefore, they had to find a solution to this problem and a method capable of finding the cheapest way to perform the entire mission or, in other terms, the way to maximise the final mass. English scientist Derek Franck Lawden's work *Optimal Trajectories for Space Navigation* [9] in 1963 has represented the opening key to the door of space optimisation and offered space scientists an important basis to start from. In this paragraph we would like to give an introduction to the Optimal Control Theory and to the steps followed in our study.

The Optimal Control Theory (OCT) [6] [7] [8] is an example of numerical analysis to perform the optimization; fields using this theory are many, due to its versatility, and space trajectories represents one of them. In Chapter 3 we will present the optimisation we have performed using this method.

OCT may be applied to a generic system of state equation(s)

$$\frac{dx}{dt} = \dot{x} = f(x, u, t) \tag{2.16}$$

where t (time) is the independent variable, x is the n-component state variables vector whereas u represents the m-component control variables vector. Usually, state equations are given together with the boundary conditions which may represent constraints imposed to the solution of the problem. Boundary conditions are usually expressed as a system of q algebraic equations (with $q \leq n + 2$) like

$$\psi\left(x_{0_j}, x_{f_j}, t_{0_j}, t_{f_j}\right) = 0 \tag{2.17}$$

The subscript "j" was introduced due to the fact that, in our study, it may be suitable to divide the trajectory into n parts (arches) chosen in order to guarantee the continuity of the variables, so that

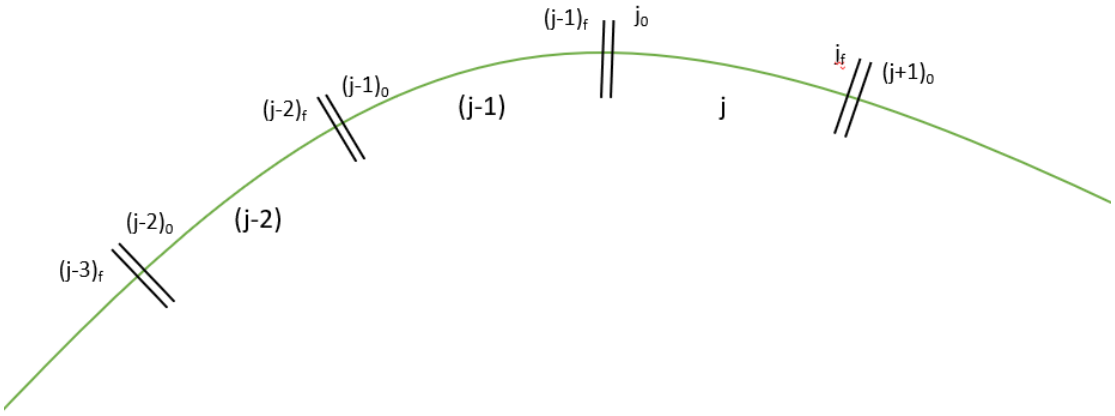

Figure 11: Subdivision of the trajectory

Subscriptions "o_j" and "f_j" indicate the start and the end of the j[th] interval.

The optimal problem consists in determining the solution $x(t)$ that maximises the function expressed by Eq. 2.16, although it is possible to consider a minimization by simply changing the sign of ϕ and φ.

$$J = \varphi\left(x_{(j-1)_+}, x_{j\_}, t_{(j-1)_+}, t_{j\_}\right) + \sum_j \int_{t_{(j-1)_+}}^{t_{j-}} \phi(x(t), u(t), t)\, dt$$

$$j = 1, \dots, n \qquad (2.18)$$

J is the sum of function φ, which depends on boundary values assumed by variables and time, and the integral, over the whole trajectory, of function ϕ expressed in terms of time, variables and controls. In our case, however, it may be useful to rewrite functional J by introducing Lagrange's multipliers:

- μ, which is a q-component vector of constants associated to the boundary conditions ψ;
- λ, which is n-component vector of adjoint variables, associated to state equations;

Hence, in this case

$$J^* = \varphi + \mu^T \psi + \sum_j \int_{t_{(j-1)_+}}^{t_{j-}} \left(\phi + \lambda^T (f - \dot{x})\right) dt$$

$$j = 1, \dots, n \qquad (2.19)$$

J and J^* depend on time, control variables, state variables and their derivatives; they are equivalent for any choice of λ and μ, assuming that boundary conditions are

satisfied. At this point, the integral can be split into three different integrals as follows:

$$\sum_j \int_{t_{(j-1)_+}}^{t_{j-}} \left(\phi + \lambda^T (f - \dot{x})\right) dt = \sum_j \int_{t_{(j-1)_+}}^{t_{j-}} \phi \, dt + \sum_j \int_{t_{(j-1)_+}}^{t_{j-}} \lambda^T f \, dt \; + \\ + \sum_j \int_{t_{(j-1)_+}}^{t_{j-}} \lambda^T \dot{x} \, dt \qquad (2.20)$$

This step allows to identify that it is possible to apply an integration by parts to the third integral so that

$$\sum_j \int_{t_{(j-1)_+}}^{t_{j-}} \lambda^T \dot{x} \, dt = \sum_j \lambda^T_{(j-1)_+} x_{(j-1)_+} - \lambda^T_{j-} x_j \; + \int_{t_{(j-1)_+}}^{t_{j-}} \dot{\lambda}^T x \qquad (2.21)$$

It is now possible to rewrite functional J^* and obtain its first order expansion:

$$\delta J^* = \left(-H_{0j} + \frac{\partial \varphi}{\partial t_{0j}} + \mu^T \frac{\partial \psi}{\partial t_{0j}}\right) \delta t_{0j} + \left(-H_{fj} + \frac{\partial \varphi}{\partial t_{fj}} + \mu^T \frac{\partial \psi}{\partial t_{fj}}\right) \delta t_{fj} \\ + \left(\lambda^T_{oj} + \frac{\partial \varphi}{\partial x_{0j}} + \mu^T \left[\frac{\partial \psi}{\partial x_{0j}}\right]\right) \delta x_{0j} + \left(\lambda^T_{fj} + \frac{\partial \varphi}{\partial x_{fj}} + \mu^T \left[\frac{\partial \psi}{\partial x_{fj}}\right]\right) \delta x_{fj} \\ + \sum_j \int_{t_{oj}}^{t_{fj}} \left(\left(\frac{\partial H}{\partial x} + \dot{\lambda^T}\right) \delta x + \frac{\partial H}{\partial u} \delta u\right) dt \qquad j = 1, \dots, n \qquad (2.22)$$

where the Hamiltonian $H = \phi + \lambda^T f$ has been introduced.

The OCT imposes that

$$\frac{d\lambda}{dt} = -\left(\frac{dH}{dx}\right)^T \tag{2.23}$$

$$\left(\frac{\partial H}{\partial u}\right)^T = 0 \tag{2.24}$$

Eq. 2.23 represents the Euler-Lagrange differential equations for the adjoint variables, whereas Eq. 2.24 are the optimal control equations. The latter means that the optimal control value is the one that nullifies the derivative of the Hamiltonian.

One last consideration needs to be done before moving on to the resolution of a boundary problem, like the one we are facing. Adjoint variables are named "free" if the corresponding state variable x is defined in one of the boundaries, such as initial or final point and they are continuous if the corresponding state variable is continuous.

In the next paragraph, we will briefly show the characteristics of a Boundary Value Problem and will present a method to solve it.

2.4 Boundary Value Problem

A Boundary Value Problem (BVP)[c] [d] consists in a system of ordinary differential equations (ODEs) whose solution and derivative values can be evaluated at more than one point. Usually, these solutions and derivatives are specified at two points *a* and *b* which represent the boundaries of the problem; this particular model of BVP is known as *two-points* BVP. A *two-point* BVP of total order n on a finite interval $[a, b]$ can be written as follows:

$$y'(x) = f\big(x, y(x)\big) \tag{2.25}$$

with

$$x \in (a, b) \qquad\qquad g\big(y(a), y(b)\big) = 0$$

where the first set of equations represents an explicit first order system of ordinary differential equations (ODEs). Functions $g(y)$ represent the n boundary conditions: they need to be independent i.e. they cannot be expressed as a function of each other. In this problem y, f and $g \in R$ and the reason of the moniker "explicit" can be easily inferred: the derivative y' appears explicitly.

However, a BVP in a form like Eq. 2.25 is quite difficult to find, since most of them arise as a combination of equations defining various orders of derivatives of the variables which sum to n.

"In an explicit BVP system, boundary conditions and right-hand sides of the equations can include the derivatives of each solution up to an order one less than the highest one of that variable appearing on the left-hand side of the ODE". (GLADWELL I, *Boundary Value Problem,* Scholarpedia, 2008)

The moniker *two-point* is given due to the boundary conditions $g(y)$, which are evaluated at the solution at the two interval endpoints a and b. If $g(y)$ is also evaluated at the solution at other points than a and b, we have a *multipoint BVP*. However, a multipoint problem may be easily converted to a two-point one by dividing the interval (a, b) in more subintervals between the points the function is evaluated in, then defining separate sets of variables for each of them and, in the end, adding boundary conditions which guarantee continuity of the variables across the whole intervals. As well as rewriting the original BVP in the compact form expressed by Eq. 2.25, converting a multipoint problem to many two-point problems may not lead to a problem with the most efficient computational solution.

Most BVPs present separated boundary conditions where the function $g(y)$ may be split into two parts (one for each endpoint):

$$g_a\big(y(a)\big) = 0 \qquad\qquad g_b\big(y(b)\big) = 0 \qquad\qquad (2.26)$$

Here, $g_a \in R^s$ and $g_b \in R^{n-s}$ for some value s, where $1 < s < n$ and where each of the vector functions g_a and g_b are independent.

Many problems have been placed in terms of BVPs in many branches of applied physics and math - for example problems involving the wave equation such as the determination of normal modes, the eigenvalues Sturm–Liouville problem - gas dynamics, nuclear physics, chemistry and study of positive radial solutions of nonlinear elliptic equations. All these BVPs could have been solved thanks to many methods developed in years, some more complex, some more easy to understand. This work made use of Genetic Algorithms (GAs)[11] [12] [13], an evolutionary search and optimisation numerical method inspired by processes normally associated with the natural world.

> "This approach is gaining a growing following in the physical, life, computer and social sciences and in engineering. Typically, those interested in GAs can be placed into one or more of three rather loose categories:
>
> 1. those using such algorithms to help understand some of the processes and dynamics of natural evolution;
> 2. computer scientists primarily interested in understanding and improving the techniques involved in such approaches, or constructing advanced adaptive systems;
> 3. those with other interests, who are simply using GAs as a way to help solve a range of difficult modelling problems." [13]

This work belongs to the last group, since GAs were used to help solving an optimization of a transfer between two different orbits.

In the next paragraph, an overview of GAs is given, along with an explanation of its mode of operation and the reasons why it needed to be developed.

2.5 The Genetic Algorithms

2.5.1 Introduction

Since the very beginning, computer scientists have built the idea of systems capable of simulating one or more of the characteristics of life. During the 50's, the idea of using a population of solutions to solve practical engineering optimisation problems was initially considered; however, GAs were conceived, invented and developed a handful of years later, by John Henry Holland, in 1972. Although these algorithms were designed for problems far more complex that those addressed in this thesis, computer scientists could improve and expand his idea to an extremely wider and wider range of problems, giving us a very powerful tool for the numerical optimisation.

GAs were born from the idea of extending the concept of natural selection and natural genetics of Charles Darwin to help solve other real-world problems.

But, what does a GA consist of?

In order to be as clearer as possible, I will summarise the contents of the first chapters of "*An Introduction to Genetic Algorithms for Scientists and Engineers*", published by David A. Coley in 1999 with World Scientific Publishing[13]: if an

interested or simply curious reader would like to deepen what is here summarised, he/she should read the entire book.

If one would like to describe how to build a genetic algorithm, he/she would probably summarise what needed as follow:

- a set, called *population*, of guesses of the solutions to the problem;
- a way of calculating the fitness of the individual solution within the population, i.e. estimate the accuracy of each term of the population;
- a method for mixing fragments of the better solutions in order to create new and, on average, even better solutions;
- a mutation operator to guarantee the continue diversity within the solutions.

By reading so few components, everyone may understand how simple a GA is, how easy its developing can be and how powerful it may be if a nowadays processor - even the most basic one - has to handle such few parameters.

2.5.2 Why do we need Genetic Algorithm?

The goal of an optimisation method is to create an infinite set of possible solutions for the analysed problem, and then search for the one that best satisfies the problem. An example might be trying to find the set of variables that, included in a mathematical model, minimise the ΔV needed for a space manoeuvre. But, what does this "search of the best solution" consist in? It is possible to measure the quality of the solution by giving it a value of success, called *fitness*, which represents its degree of accuracy. Better/poorer performing solutions will then represent the closest points to the maximum/minimum within the search space (or fitness landscape). If more than one variable is considered, then the goal of the algorithms is to find the combination that gives the highest fitness value, which does not always correspond to the set of best solutions. Furthermore, those spaces or landscapes can be of surprising complexity: in fact, even for simple problems, they can show numerous peaks of varying heights, separated from each other by valleys on all scales. The highest peak is usually referred to a global maximum, the lesser peaks to local maxima. Usually, the scope of using genetic algorithms is to find out the global optimum (i.e. maximum or minimum) solution, but this need not be so. Sometimes, for example in real-time control, in architectural design or aerospace structures, it is necessary to determine the first point which exceeds certain value, but it may not be the global optimum.

To understand why GA were introduced, it may be important to figure out why many traditional algorithms can encounter difficulties, when searching such spaces for the global optimum. Figure 12 shows experimental measurements of a dependent variable y that have been made at various points j of the independent variable x, demonstrating a mutual relationship between x and y values, such as

$$y = mx + c \tag{2.27}$$

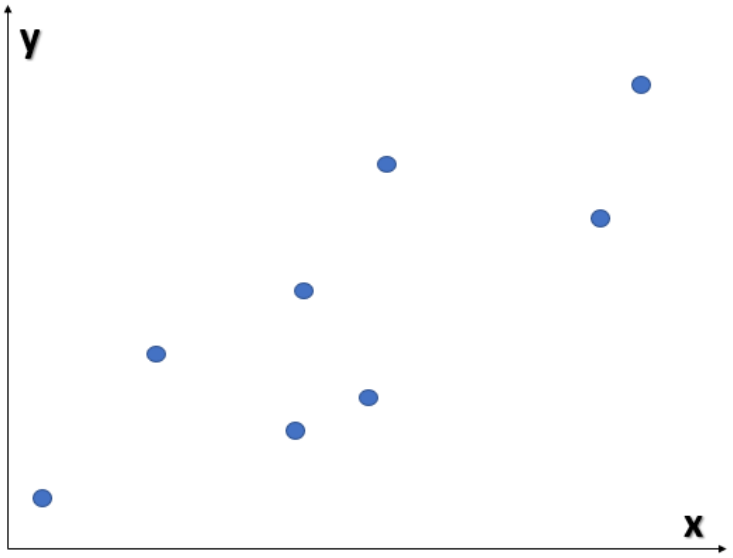

Figure 12: Feasible experimental values for an example function y=mx+c

One of the most common numerical ways of finding the best estimate of m is by using a least-squares estimation. In this technique, the error between y (predicted solution using Eq. 2.27) and $\bar{y}$ (measured solution during the experiment), can be expressed by a least squares cost function Ω :

$$\Omega = \sum_{j=1}^{n} \left(\bar{y}_j - y_j\right)^2 \tag{2.28}$$

where n is the number of data points.

Expanding Eq. 2.28 gives:

$$\Omega = \sum_{j=1}^{n} \left(\bar{y}_j - (mx_j + c)\right)^2 \tag{2.29}$$

This method simply evaluates the sum of the squares of the vertical distances between y and $\bar{y}$ (see Figure 13). The function Ω will be minimized as soon as this sum will reach a minimum; therefore, a smart approach could be to evaluate Ω for a large set of values of m and then identify the one that gives the lowest estimation.

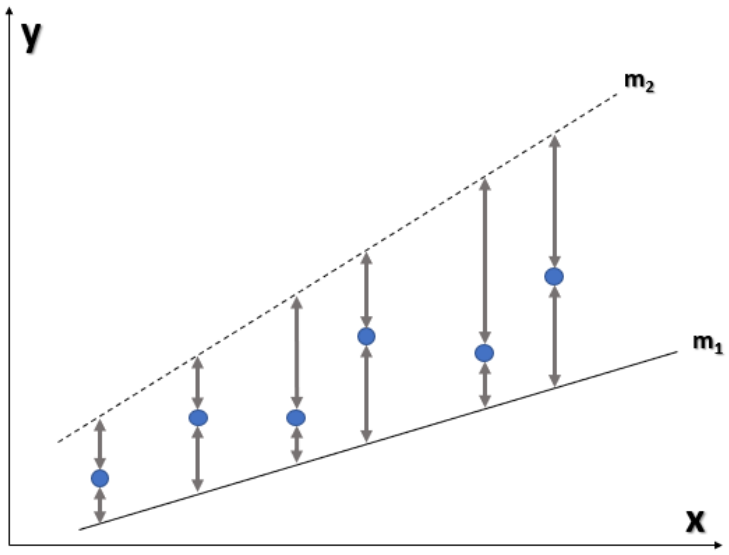

Figure 13: Vertical distances between two values of m

This procedure and this case are very easy, but it is even easier to understand that things may get really much complicated if the number of variables increases. Something not easy to understand, instead, is that they can get worse even with still one variable.

Let's take a look at Figure 14.

This represents the evolution of Ω with respect to m. In order to identify the value of m that minimises Ω, a feasible approach may be to guess two possible values of m (m_1 and m_2), then if $\Omega(m_1) > \Omega(m_2)$, it is possible to discard m_1 and make the next guess at some point m_3 where $m_3 = m_2 + \delta$, or else head the other way. Given some suitable, dynamic, way of adjusting the value of δ, the method will rapidly settle on m^* (i.e. the global minimum).

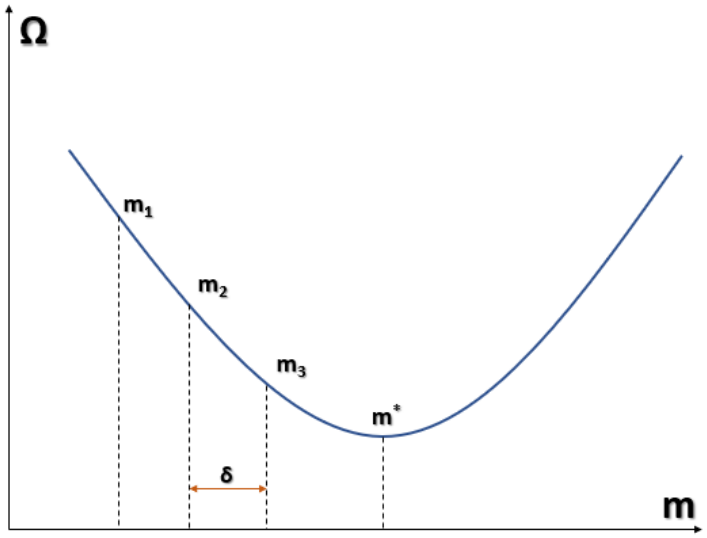

Figure 14: Steps of the evaluation of the best value of m

This approach is described as a direct search (because it does not make use of derivatives or other information) and it can be very efficient. But what happens if we have a function like the one shown in Figure 15?

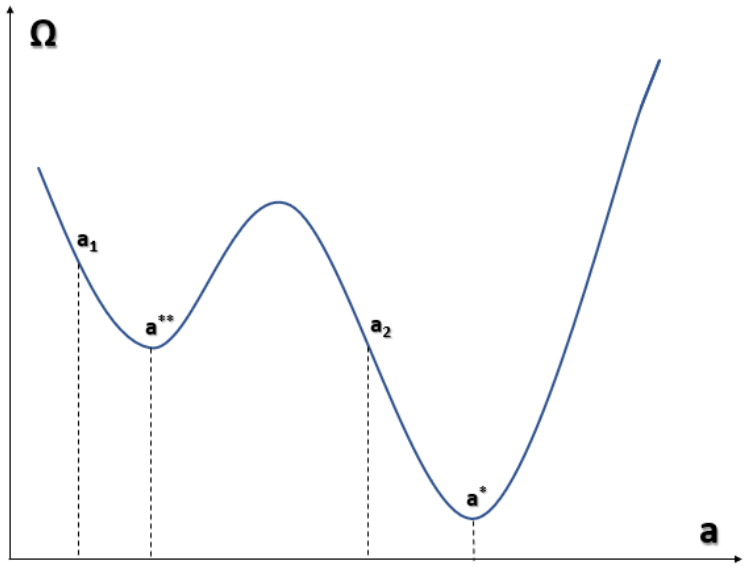

Figure 15: Steps of the evaluation of the best value of a

If either the direct search algorithm outlined above or a simple calculus-based approach is used, the final estimation of a will depend on the starting point of the algorithm. Making the initial guess at $a = a_2$, will indeed lead to the correct (global) minimum, a^*; however, if $a = a_1$ is used then only a^{**} will be reached (local minimum). It is not difficult now to imagine how complex a multi-variable problem can be.

Here, GA comes to help us. The basic idea is that GA chooses a set of values of the variables within a given interval, evaluates the value of Ω for each of them, memorising the best one, then it chooses another set of values and repeats this cycle until it finds the global minimum.

But let's see its mode of operation more in detail.

2.5.3 How does it work?

Rather than starting from a single point (or guess) within the search space, as said before, GA starts working with a population of guesses. The user gives as input a range of values among which the algorithm may choose the initial and the following guesses of the unknown variables. Typically, these initial guesses arise as binary strings of the true variables, although an increasing number of GAs uses "real-valued" (i.e. base-10) encodings. After the initial guess, the algorithm uses three different operators to evaluate a new population of guesses, driving the problem to converge at the global optimum. These operators are: selection, crossover and mutation (as one can observe, the names are analogous to the natural world).

Selection seeks to simulate natural selection found in biological systems: a fitness value is assigned to each solution, so that poorer performing individuals are discarded whether better ones have a greater than average chance of promoting the information they contain within the next generation.

Crossover acts like the recombination mechanism belonging to the human reproduction: it deals with the transfer of characteristics from parents to children. The most common method to realise that is called *single point crossover* (SPC). SPC consists in choosing pairs of individuals promoted by the selection operator (possibly of equal length), randomly determine a single locus (point) within the binary strings where the crossover will occur and then swap all the information

(digits) to the right of this locus between the two individuals (the example in the next paragraph will clarify this process).

Mutation is, at the same time, the most important and the rarest operator (it is applied more or less to one bit in every thousand): its task is to randomly change (flip) the value of single bits within individual strings. The role of the mutation is a key one due to the fact that it is charged with maintaining the genetic diversity of the population. Without it, probably most GAs would not converge to the optimum.

After selection, crossover and mutation have been applied to the initial population, a new population is generated, and this process continues until one of the stopping criteria have been fulfilled. Example of stopping criteria might be: maximum number of generations, maximum elapsed time, minimum tolerance of fitness value etc.

2.5.4 An example

Before start using GA, many things need to be specified, e.g. the method of encoding the unknown parameters (as binary strings, base-10 numbers, etc.), the population size, how to apply the concept of mutation to the representation, the stopping criteria. Once all these options are set, GA can start the process of optimisation.

We are going to address the minimisation of the example function:

$$y = 3x^2 + 5 \tag{2.30}$$

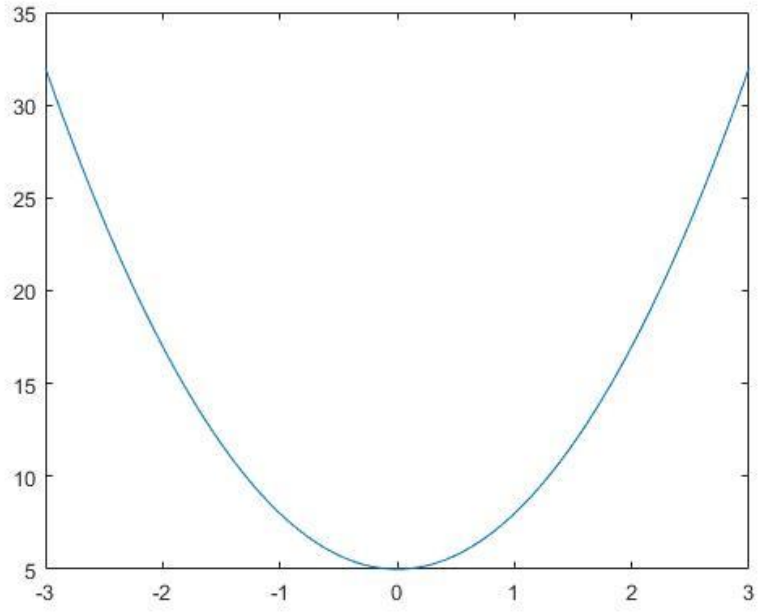

Figure 16: Evolution of example function y

Obviously, the answer to our problem is $x = 0$ but we want the genetic algorithm to find the solution for us: therefore, we will now follow its mode of operation step by step:

1. GA makes a set (eight for this example) of guesses, randomly choosing within the range given by the user (for example $0 \leq x \leq 3500$);

2. It tests these guesses as solutions of the function and assigns a fitness value to each of them: since our problem is a minimisation problem, the lower is the resulting y, the higher is the fitness value;

Population Number	X	Binary String	Fitness
1	125	000001111101	2133,106
2	2889	101101001001	3,993
3	548	001000100100	110,998
4	19	000000010011	91911,76
5	1237	010011010101	21,784
6	356	000101100100	263,01
7	88	000001011000	4303,482
8	3284	110011010100	3,091

Table 1: Fitness values of initial guesses

3. It identifies the best half (those with highest fitness, yellow highlighted) and converts them to binary strings (bold values);

4. It then randomly selects pairs of parents from the best half (we choose 1 with 7 and 4 with 6 referring to table 1) and undergoes them a single point crossover.

Binary Parents Strings	Children	Numerical Children	Fitness
0000011/11101	000001011101	93	3853,268
0000010/11000	000001111000	120	2314,547
000000010/011	000001011011	91	4024,469
000001011/000	000000010000	16	129366,1

Table 2: Children of initial guesses

5. It applies mutation to the children by occasionally changing a 0 to 1 or vice versa: for example, if it is applied to the sixth bit of the second child (120) it becomes 111000, which corresponds to 56;

6. It puts together the four children with the four parents belonging to the group of the best half to form the new population, which still consists of 8 elements;

Population Number	x	Fitness	Binary String
1	125	2133,106	000001111101
2	19	91911,76	000000010011
3	356	263,01	000101100100
4	88	4303,482	000001011000
5	93	3853,268	000001011101
6	120	2314,547	000001111000
7	91	4024,469	000001011011
8	16	129366,1	000000010000

Table 3: New Population

7. It repeats steps 2-7 until stopping conditions is reached.

A brief further consideration needs to be done about the importance of mutation. Consider this group of parents, chosen as best values from the initial population (this example is not related to the previous one):

000101

010101

001111

001000

As one can observe, each of the values starts with "0"; that means that, from this generation until the end, no "1" will appear in first position and this could be a very big problem if, for example, the global optimum has $x > 111111 = 63$. Mutation would replace one of the zeros with a "1" and this would guarantee a presence of "1" in the future generations as well as reaching of the global optimum.

2.6 The function *fminsearch*

fminsearch is a MATLAB function that allows the user to find a local minimum of an unconstrained non-linear problem like

$$\begin{cases} \min f(x) \\ c(x) = 0 \end{cases} \tag{2.31}$$

where $f: R^n \to R$ is the objective function and $c(x) = 0$ represents a (or a set of) constraint equation(s).

Its syntax is very simple: it needs as inputs the function to minimise, the initial guesses to start the algorithm and, eventually, a vector with the options we would like to modify from the default ones. In this work only two options have been modified: the output, since we wanted a plot of the function values during the algorithm run like the one in Figure 17 (Chapter 3), and the tolerance of the function value (changed from 10^{-4} to 10^{-6} for a more accurate solution).

One can ask himself what is the difference with respect to GA? The answer is very simple, though.

fminsearch is very powerful because it converges very quickly to the solution but has the big limitation of converging to a minimum, which may be a global or a local

one: in fact, it converges to the closest minimum from the initial guesses we give as inputs. We do not have any assurance that the minimum found by the function matches the global optimum we are looking for.

This is why, in this work, we used them both: GA guarantees ***fminsearch*** an initial guesses close enough to the global optimum so that we are sure that the function converges to the point we need.

fminsearch is based on a very successful method for solving nonlinearly constrained optimization problems called *Sequential Quadratic Programming* (SQP)[15]". Like GA, SQP became popular in the 1970s but it is not only an algorithm, but rather a basic conception from which numerous other specific algorithms have been evolved. Based on a solid theoretical and computational foundation, SQP algorithms have been developed and used to solve a remarkably large set of important practical problems. In the next paragraph an overlook of the SQP is given but it won't be as detailed as the one for GA since SQP plays a very secondary role in this work.

2.6.1 Sequential Quadratic Programming

The real goal of a Sequential Quadratic Programming algorithm is to model the problem shown in Eq. 2.31 at a given approximate solution, for example x^j, through a quadratic programming subproblem, and then to use the solution to this subproblem to find a better approximation x^{j+1}. This process is then iterated to create a sequence of approximations that will hopefully converge to the solution x^*.

Probably the easiest way to catch on the mode of operation and basics of SQP is the fact that, with an appropriate choice of quadratic subproblem, the method can be seen as the natural extension of Newton and quasi-Newton methods. However, SQP algorithms present themselves to be really more complex than Newton methods due, most of all, to the presence of constraints.

One last key property of the SQP method should be pointed out.

SQP is not a feasible-point method; that is, the initial point nor any of the subsequent iterates need to satisfy the constraints (i.e. be feasible). It is quite obvious that this represents a crucial advantage, since finding a feasible point with nonlinear constraints may be nearly as hard as solving the problem itself.

What SQP does is to assume a second-order expansion for $f(x)$ and a first-order expansion for the constraints $c(x)$ (we consider x as a vector of state variables $x_1, x_2, \dots, x_n$):

$$\begin{cases} f(x+\Delta x) = f(x) + g^T \Delta x + \frac{1}{2}\Delta x^T [H] \Delta x \\ \\ c(x+\Delta x) = c(x) + [G]\Delta x \end{cases} \tag{2.32}$$

where

$$g^T = \frac{\partial f}{\partial x_i} = \left(\frac{\partial f}{\partial x_1}, \frac{\partial f}{\partial x_2}, \dots, \frac{\partial f}{\partial x_n}\right) \tag{2.33}$$

$$[H] = \begin{bmatrix} \frac{\partial^2 f}{\partial x_1 \partial x_1} & \frac{\partial^2 f}{\partial x_1 \partial x_2} & \dots & \frac{\partial^2 f}{\partial x_1 \partial x_n} \\ \frac{\partial^2 f}{\partial x_2 \partial x_1} & \frac{\partial^2 f}{\partial x_2 \partial x_2} & \dots & \frac{\partial^2 f}{\partial x_2 \partial x_n} \\ \dots & \dots & \dots & \dots \\ \frac{\partial^2 f}{\partial x_n \partial x_1} & \frac{\partial^2 f}{\partial x_n \partial x_2} & \dots & \frac{\partial^2 f}{\partial x_n \partial x_n} \end{bmatrix} \tag{2.34}$$

$$[G] = \begin{bmatrix} \frac{\partial c_1}{\partial x_1} & \frac{\partial c_1}{\partial x_2} & \dots & \frac{\partial c_1}{\partial x_n} \\ \frac{\partial c_2}{\partial x_1} & \frac{\partial c_2}{\partial x_2} & \dots & \frac{\partial c_2}{\partial x_n} \\ \dots & \dots & \dots & \dots \\ \frac{\partial c_n}{\partial x_1} & \frac{\partial c_n}{\partial x_2} & \dots & \frac{\partial c_n}{\partial x_n} \end{bmatrix} \tag{2.35}$$

g represents the gradient of f (n-component vector) while $[H]$ represents the Hessian of f ($n\ x\ n$ symmetric matrix) and $[G]$ the Jacobian of constraint equations c_i ($m\ x\ n$ matrix).

Note that a linear approximation is implicitly adopted for the gradient, so that

$$g(x + \Delta x) = g(x) + [H]\Delta x \tag{2.36}$$

Using Newton's method together with a particular set of equations named Kuhn-Tucker equations (more details can be found in [10]), SQP starts an iterative procedure with the goal to find the final solution which, as said before, may not coincide with the global minimum if the initial guess(-es) is (are) not close enough.

2.7 References

2.7.1 Bibliography

1. BONAVITO N. L., DER G. J., VINTI J. P., "*The Lagrange Planetary Equations", Orbital and Celestial Mechanics*, Progress in Astronautics and Aeronautics, 1998

2. CORNELLISSE J.W., SCHOYER H.F.R., WAKKER K. F., *Rocket Propulsion and Spaceflight Dynamics,* Pitman, London, 1979

3. EDELBAUM N. THEODORE, *Propulsion Requirements for Controllable Satellites",* ARS Journal Vol. 31, Aug 1961

4. CASALINO L., COLASURDO G., *Improved Edelbaum's Approach to Optimize Low Earth/Geostationary Orbits Low - Thrust Transfers,* Journal of Guidance, Control and Dynamics, Vol 30, Sept/Oct 2007

5. MOULTON F.R., *Celestial Mechanics,* The Macmillan Company, 1914

6. KIRK E.D., *Optimal Control Theory An Introduction,* Prentic Hall INC, 1971

7. TEODOROV E., *Optimal Control Theory,* MIT Press, 2006

8. EVANS L.C., *An Introduction to Mathematical Optimal Control Theory,* 1985

9. LAWDEN D.F., *Optimal Trajectories For Space Navigation,* Butterworth and Co.,1963

10. WALLACE B., *Constrained Optimization: Kuhn-Tucker conditions*, Economy Dept, 2004

11. PANICUCCI B., PAPPALARDO M., PASSACANTANDO M., *Introduzione all'optimisatioin toolbox di Matlab*

12. TAVAKOLI A., PLANTE D., *Solving Boundary Value Problems by Genetic Algorithm,* 2016

13. COLEY D. A., *An Introduction to Genetic Algorithms for Scientists and Engineers,* World Scientific Publishing, 1999

14. ARQUB O.A., ABO-HAMMOUR Z., MOMANI S., SHAWAGFEH H., *Solving Singular Two-Point Boundary Value Problem Using Continuous Genetic Algorithm,* Hindawi Publishing, 2012

15. BOGGS P. T., TOLLE J. W., *Sequential Quadratic Programming*, Acta Numerica, 1996

16. AVANZINI G., COLASURDO G., *Astrodynamics,* Politecnico di Torino, 2006

2.7.2 Sitography

a) *astronomy.stackexchange.com/questions/18761/j2-perturbations-and-orbits*

b) *www.aerospacengineering.net/?p=537*

c) *www.scholarpedia.org/article/Boundary_value_problem*

d) *users.math.msu.edu/users/sen/math_235/lectures/lec_20_fs12_bvp.pdf*

e) *www.scholarpedia.org/article/Initial_value_problem*

Chapter 3:

The Results

The goal of this chapter is to summarise the outcome of our work. Its structure is very simple: we will first apply step by step the theory explained in the previous chapter and then present the analytical and graphical results.

As shown in Chapter 1, we have considered a default setup of the S/C that performs the manoeuvre, in order to give specific numerical results and offer a better overview of them, but it is clearly possible to modify the parameters, customising the study as needed.

We first adapted Edelbaum equations for our study, then performed an optimisation for both a one-revolution transfer and a multi-revolution transfer, obtaining important analytical results. At a later time, these differential equations were given as an input to a MATLAB script, compiled in order to use Genetic Algorithm and

fminsearch: their goal is to find the optimal result (global minimum) that nullifies the error over the imposed final conditions and the boundary ones by minimising an appropriate function. The results show the evolution of our variables in time that represents the way to perform the manoeuvre. Finally, we ran different simulations by changing the initial conditions, in order to obtain a wide range of solutions and capture a variety of scenarios.

3.1 The Optimisation of the Manoeuvre

3.1.1 One Revolution Transfer Optimisation

The first step of this chapter is to present the optimisation of the Edelbaum equations (Eq. 2.6) for a one-revolution transfer to obtain the variation of the Keplerian elements after one revolution around the Earth.

The first step is defining some assumptions we have done:

- $e \sim 0$, since we consider quasi circular orbit: this allowed us to neglect the variation of the eccentricity e and the argument of periapsis ω;
- $\theta = \omega + \nu$, defined as the angular distance from the ascending node;
- a (Semimajor axis) = r (position vector) = p (semilatus rectum), since the eccentricity is equal to zero; $d\theta/dt = \sqrt{\mu/a^3}$
- V is the orbital velocity defined by:

$$V = \sqrt{\frac{\mu}{a}}\ ; \tag{3.1}$$

- The accelerations are defined by:

$$A_v = A\ cos\ \beta, \quad A_w = A \sin \beta\ ; \tag{3.2}$$

Hence, we obtain:

$$\begin{aligned}
\frac{da}{dt} &= \frac{2Aa^2}{\sqrt{\mu a}}\cos\beta \\
\frac{di}{dt} &= \sqrt{\frac{a}{\mu}}Asin\beta\cos\theta \\
\frac{d\Omega}{dt} &= \sqrt{\frac{a}{\mu}}A\left(\frac{sin\beta}{\sin i}\right)\sin\theta - \frac{3}{2}j_2\left(\frac{R_e}{a}\right)^2\sqrt{\frac{\mu}{a^3}}\cos i \\
\frac{d\theta}{dt} &= \sqrt{\frac{\mu}{a^3}}
\end{aligned} \tag{3.3}$$

At this point, it can be useful to change the independent variable from time to θ so that we can then easy integrate from 0 to 2π. To make this change:

$$\frac{dx}{d\theta} = \frac{dx}{dt}\cdot\frac{dt}{d\theta} \tag{3.4}$$

Hence, we have:

$$\begin{aligned}
\frac{da}{d\theta} &= \frac{2Aa}{\mu/a^2}\cos\beta \\
\frac{di}{d\theta} &= \frac{A}{\mu/a^2}sin\beta\cos\theta \\
\frac{d\Omega}{d\theta} &= \frac{A}{\mu/a^2}\left(\frac{sin\beta}{\sin i}\right)\sin\theta - \underline{\frac{3}{2}j_2\left(\frac{R_e}{a}\right)^2\cos i} \\
\frac{dt}{d\theta} &= \sqrt{\frac{a^3}{\mu}}
\end{aligned} \tag{3.5}$$

Particular attention must be given to the third equation. The underlined term is the contribution of the perturbation j_2 that we add to the equation to take it into account. As we mentioned in the previous chapter, the effect is relevant only with RAAN, whereas is negligible or totally absent for the other Keplerian elements.

At this point it is possible to perform the optimisation.

We have to predefine the control vector u and the state vector x :

$$u = [\beta]$$

$$x = [a, i, \Omega, \mathrm{t}]$$

where $\beta = steering\ angle$.

We can now define the Hamiltonian as:

$$H = \sum_x \lambda_x \frac{\partial x}{\partial \theta} \tag{3.6}$$

However, since we are considering one revolution,

$$\begin{cases} a \sim a_0 \\ i \sim i_0 \end{cases}$$

Therefore

$$\dot{\lambda_x} = -\frac{\partial H}{\partial x} = 0 \quad , \quad \lambda_x = cost \tag{3.7}$$

λ_x are very important parameters representing the gain associated with changing x; thus, the higher are their absolute values, the greater is the gain.

With this assumption, Eq. 2.23 is solved, and we need to face Eq. 2.24.

The optimum value of β is the one that nullify the derivatives of the Hamiltonian:

$$\frac{\partial H}{\partial \beta} = 0 \tag{3.8}$$

Solving Eq. 3.8, we obtained:

$$\tan\beta = \frac{\lambda_i \cos\theta + \frac{\lambda_\Omega \sin\theta}{\sin i}}{2\lambda_a a} \tag{3.9}$$

$$\tan\theta_0 = \frac{\lambda_\Omega}{\lambda_i \sin i} \tag{3.10}$$

We can introduce some parameters, such as

$$\Lambda = \sqrt{\left(\frac{\lambda_\Omega}{\sin i}\right)^2 + \lambda_i^2} \tag{3.11}$$

$$K = \frac{\Lambda}{2a\lambda_a} \tag{3.12}$$

Hence, Eq. 3.9 can be rewritten:

$$\tan\beta = \cos(\theta - \theta_0) \tag{3.13}$$

It is useful to perform a change of variables as follow:

$$\theta' = \theta - \theta_0 \tag{3.14}$$

So that:

$$\tan\beta = K\cos\theta' \tag{3.15a}$$

$$\sin\beta = \frac{K\cos\theta'}{\sqrt{1+(K\cos\theta')^2}} \tag{3.15b}$$

$$\cos\beta = \frac{1}{\sqrt{1+(K\cos\theta')^2}} \tag{3.15c}$$

If we then define

$$R = \sqrt{1+(K\cos\theta')^2} \tag{3.16}$$

it is possible to rewrite Eq. 3.5 as:

$$\begin{aligned}
\frac{da}{d\theta'} &= \frac{da}{d\theta} = \frac{2A}{\mu/a^2}a\frac{1}{R} \\
\frac{di}{d\theta'} &= \frac{di}{d\theta} = \frac{A}{\mu/a^2}\frac{K\cos\theta'}{R}\cos(\theta'+\theta_0) \\
\frac{d\Omega}{d\theta'} &= \frac{d\Omega}{d\theta} = \frac{A}{\mu/a^2}\left(\frac{K}{\sin i}\right)\frac{\cos\theta'}{R}\sin(\theta'+\theta_0) - \frac{3}{2}j_2\left(\frac{R_e}{a}\right)^2\cos i \\
\frac{dt}{d\theta'} &= \frac{dt}{d\theta} = \sqrt{\frac{a^3}{\mu}}
\end{aligned} \tag{3.17}$$

Now we should integrate these equations from 0 to 2π. Edelbaum also did this, assuming $\theta_0 = 0$ though: in fact, he considered the case of negligible inclination, for which Ω has no meaning.

In addition, we note that:

$$\int_0^{2\pi} \frac{\sin\theta'\cos\theta'}{R}d\theta' = 0 \tag{3.18}$$

Consequently, we find out that our results are very close to Edelbaum's. In fact, if the index 0 refers to Edelbaum's solutions, we have:

$$\begin{aligned} \Delta a &= \Delta a_0 \\ \Delta i &= \Delta i_0 \cos\theta_0 \\ \Delta\Omega &= \frac{\Delta i_0 \sin\theta_0}{\sin i} \\ \Delta t &= \Delta t_0 \end{aligned} \tag{3.19}$$

Edelbaum's solutions, however, are not so simple to calculate, therefore it may be useful to consider a simplified solution assuming $\beta = \pm K$ where the sign changes for $\theta_0 = \frac{\pi}{2}$. Under this assumption:

$$\int_{1rev} \frac{dx}{d\theta} d\theta = 2 \int_{\theta_0-\frac{\pi}{2}}^{\theta_0+\frac{\pi}{2}} \frac{dx}{d\theta} d\theta \tag{3.20}$$

Hence, we obtain:

$$\boxed{\boldsymbol{\Delta a} = \frac{2A}{\mu/a^2} \mathrm{a}\cos\beta \int_0^{2\pi} d\theta = \frac{\boldsymbol{4\pi A}}{\frac{\boldsymbol{\mu}}{\boldsymbol{a^2}}} \mathbf{a}\cos\boldsymbol{\beta}}$$

$$\boxed{\boldsymbol{\Delta i} = \frac{2A}{\mu/a^2} \sin\beta \int_{\theta_0-\frac{\pi}{2}}^{\theta_0+\frac{\pi}{2}} \cos\theta\, d\theta = \frac{\boldsymbol{4A}}{\frac{\boldsymbol{\mu}}{\boldsymbol{a^2}}} \sin\boldsymbol{\beta}\cos\boldsymbol{\theta_0}} \tag{3.21}$$

$$\boxed{\boldsymbol{\Delta\Omega} = \frac{2A}{\mu/a^2} \sin\beta \int_{\theta_0-\frac{\pi}{2}}^{\theta_0+\frac{\pi}{2}} \sin\theta\, d\theta - (\dots) = \frac{\boldsymbol{4A}}{\frac{\boldsymbol{\mu}}{\boldsymbol{a^2}}} \frac{\sin\boldsymbol{\beta}}{\sin\boldsymbol{i}} \sin\boldsymbol{\theta_0} - \boldsymbol{3\pi j_2}\left(\frac{\boldsymbol{R_e}}{\boldsymbol{a}}\right)^2 \cos\boldsymbol{i}}$$

$$\boxed{\boldsymbol{\Delta t} = T = \boldsymbol{2\pi}\sqrt{\frac{\boldsymbol{a^3}}{\boldsymbol{\mu}}}}$$

These equations express the variation of the orbital elements after a single revolution. As we can see, the term of j_2 has remained the same throughout all the steps, since it is not function of θ.

Also, it can be noticed that these equations follow the laws expressed by Eq. 3.19 perfectly. This means that, even if we are considering also a change of RAAN (different to Edelbaum), we can still assume a constant value of β (like Edelbaum) changing sign according to the sign of $(\theta - \theta_0)$.

It is now possible to combine these results to obtain those for the multirevolution transfer.

3.1.2 Multirevolution Transfer Optimisation

Two different approaches may be used in this analysis.

The first consists of using the Semimajor axis as independent variable, (similarly to Edelbaum's), whereas the second uses time. We will see that the latter is the most convenient choice that we have used to calculate the following steps.

Using the Semimajor axis a as independent variable, we need to derive the variation of the other elements as

$$\frac{dx}{da} \approx \frac{\Delta x}{\Delta a} \tag{3.22}$$

Hence, we have,

$$\begin{aligned} \frac{d\Omega}{da} &= \frac{\tan\beta \sin\theta_0}{\pi\, a \sin i} - \frac{3}{4} \frac{j_2 \left(\frac{R_e}{a}\right)^2 \cos i}{A \cos\beta} \frac{\mu}{a^3} \\ \frac{di}{da} &= \frac{\tan\beta \cos\theta_0}{\pi\, a} \\ \frac{dt}{da} &= \frac{\sqrt{\frac{\mu}{a^3}}}{2A\cos\beta} \end{aligned} \tag{3.23}$$

We can now perform the optimisation by deriving the Hamiltonian as expressed by Eq. 3.6. This time, only λ_Ω and λ_t are constant.

In fact

$$\dot{\lambda}_\iota = \lambda_\Omega \left(\frac{\tan\beta \sin\theta_0 \cos i}{\pi\, a \sin^2 i} - \frac{3}{4} \frac{j_2 \left(\frac{R_e}{a}\right)^2 \sin i}{A \cos\beta} \frac{\mu}{a^3} \right) \tag{3.24}$$

Here, one can observe that the smaller is the inclination, the higher is the advantage in changing Ω.

In order to find the optimal controls – this time $u = [\beta, \theta_0]$ – we need to calculate the derivatives of the Hamiltonian with respect to the control parameters and then find the values that nullify them.

$$\frac{\partial H}{\partial \theta_0} = \frac{\lambda_\Omega \cos\theta_0}{\sin i} - \lambda_i \sin\theta_0 = 0 \tag{3.25}$$

Solving Eq. 3.25 in terms of θ_0, we find

$$\tan\theta_0 = \frac{\lambda_\Omega}{\lambda_\mathrm{i} \sin i} \tag{3.26}$$

Even though Eq. 3.26 appears to be the same as Eq. 3.10, the difference between the two consists in a different meaning of λ_x: in Eq. 3.10 they were intended over a single revolution whereas in Eq. 3.26 over a multiple revolution. With Eq. 3.26, moreover, there are additional troubles. In order to find θ_0 we should use the arctangent, that would give us two solutions (first and third quadrant or fourth and second) and choose between them. However, OCT imposes that the optimal control both nullify the derivatives of the Hamiltonian and maximise it. Consequently, it is

necessary to choose the right solution and figure out the one that correspond to the maximum.

Deriving the second optimum control value:

$$\frac{\partial H}{\partial \beta} = 0 = \left(\frac{\lambda_\Omega \sin\theta_0}{\pi \operatorname{asin} i} + \frac{\lambda_i \cos\theta_0}{\pi a}\right)\frac{1}{\cos^2\beta} + \left(\frac{\sqrt{\frac{\mu}{a^3}}}{2A} - \lambda_\Omega \frac{3}{4}\frac{j_2\left(\frac{R_e}{a}\right)^2 \cos i}{A}\frac{\mu}{a^3}\right)\frac{\sin\beta}{\cos^2\beta} \tag{3.27}$$

Solving, we have

$$\sin\beta = \frac{\Lambda}{\pi a}\cdot\frac{2A}{-\lambda_t\sqrt{\frac{\mu}{a^3}} + \frac{3}{2}j_2\left(\frac{R_e}{a}\right)^2 \cos i\ \frac{\mu}{a^3}} \tag{3.28}$$

Where Λ is expressed by Eq. 3.11.

With Eq. 3.28 it is easily understandable that by arbitrarily choosing a value of $\sin\beta$ the corresponding value of θ_0, which maximises the Hamiltonian, has the same sign. Therefore, for simplicity, we consider a positive value of $\sin\beta$ so that all the signs are positive.

This approach, as we previously explained, is quite intricate because it is difficult to know the type of mission we are going to face a priori: we do not know if it is, for example, more convenient to first increase the Semimajor axis and then decrease it or vice versa or even to decrease it directly.

This is the reason why we opted for the second approach, assuming time as independent variable. Since time is always positive, the problem does not arise anymore.

The steps are the same of the previous approach.

We define the variation of the elements, referring now to time.

$$\frac{dx}{dt} \approx \frac{\Delta x}{\Delta t} \tag{3.29}$$

Therefore, we have:

$$\boldsymbol{\frac{da}{dt}} \approx \frac{\Delta a}{\Delta t} = 4\pi A a \cos\beta \sqrt{\frac{a^2}{\mu}} \frac{1}{2\pi} \sqrt{\frac{\mu}{a^3}} = \boldsymbol{\frac{2A}{\sqrt{\mu}} a^{\frac{3}{2}} \cos\beta}$$

$$\begin{aligned} \boldsymbol{\frac{d\Omega}{dt}} \approx \frac{\Delta\Omega}{\Delta t} &= \frac{4Aa^2}{\mu} \frac{\sin\beta}{\sin i} sin\theta_0 \frac{1}{2\pi} \sqrt{\frac{\mu}{a^3}} - \frac{3\pi}{2\pi} j_2 \left(\frac{R_e}{a}\right)^2 \cos i \sqrt{\frac{\mu}{a^3}} \\ &= \boldsymbol{\frac{2A\sqrt{a}}{\pi\sqrt{\mu}} \frac{\sin\beta}{\sin i} sin\theta_0 - \frac{3}{2} j_2 \frac{R_e^2}{a^{\frac{7}{2}}} \cos i \sqrt{\mu}} \end{aligned} \tag{3.30}$$

$$\boldsymbol{\frac{di}{dt}} \approx \frac{\Delta i}{\Delta t} = \frac{4Aa^2}{\mu} \sin\beta \, cos\theta_0 \frac{1}{2\pi} \sqrt{\frac{\mu}{a^3}} = \boldsymbol{\frac{2A\sqrt{a}}{\pi\sqrt{\mu}} \sin\beta \, cos\theta_0}$$

We can now define the Hamiltonian as

$$\begin{aligned} H = \lambda_a \left(\frac{2A}{\sqrt{\mu}} a^{\frac{3}{2}} \cos\beta\right) + \lambda_\Omega \left(\frac{2A\sqrt{a}}{\pi\sqrt{\mu}} \frac{\sin\beta}{\sin i} sin\theta_0 - \frac{3}{2} j_2 \frac{R_e^2}{a^{\frac{7}{2}}} \cos i \sqrt{\mu}\right) \\ + \lambda_i \left(\frac{2A\sqrt{a}}{\pi\sqrt{\mu}} \sin\beta \, cos\theta_0\right) \end{aligned} \tag{3.31}$$

First of the following steps is to derive the variations $\dot{\lambda_x}$; hence

$$\dot{\lambda_a} = -\frac{\partial H}{\partial a} = -\left[\lambda_a \frac{3A}{\sqrt{\mu}}\sqrt{a}\cos\beta + \lambda_\Omega\left(\frac{A}{\pi\sqrt{\mu}}\frac{\sin\beta}{\sin i}\frac{sin\theta_0}{\sqrt{a}} - \frac{21}{4}j_2\frac{R_e^2}{a^{\frac{9}{2}}}\cos i\ \sqrt{\mu}\right) + \lambda_i\left(\frac{A}{\pi\sqrt{\mu}}\frac{1}{\sqrt{a}}\sin\beta\ cos\theta_0\right)\right]$$

$$\dot{\lambda_\Omega} = 0 \tag{3.32}$$

$$\dot{\lambda_\imath} = -\lambda_\Omega\left(-\frac{2A\sqrt{a}}{\pi\sqrt{\mu}}\frac{\sin\beta}{\sin^2 i}\cos i\ sin\theta_0 + \frac{3}{2}j_2\frac{R_e^2}{a^{\frac{7}{2}}}\sin i\ \sqrt{\mu}\right)$$

Successively, we have to determine the optimal control values i.e. those that nullify the derivatives of the Hamiltonian:

$$\frac{\partial H}{\partial \theta_0} = \frac{\lambda_\Omega\cos\theta_0}{\sin i} - \lambda_i\sin\theta_0 = 0 \tag{3.33}$$

Solving Eq. 3.33 in terms of θ_0, we find

$$\tan\theta_0 = \frac{\lambda_\Omega}{\lambda_\imath\sin i} \tag{3.34}$$

We can then easily define

$$\sin\theta_0 = \pm\frac{\lambda_\Omega}{\Lambda\sin i}$$
$$\cos\theta_0 = \pm\frac{\lambda_i}{\Lambda} \tag{3.35}$$

that represent the same results of the previous approach. Changes will be seen immediately.

In fact, the partial derivative of the Hamiltonian with respect to β is

$$\frac{\partial H}{\partial \beta} = -\lambda_a \frac{\cancel{2A\sqrt{a}}}{\cancel{\pi\sqrt{\mu}}} \pi a \sin\beta + \lambda_\Omega \frac{\cancel{2A\sqrt{a}}}{\cancel{\pi\sqrt{\mu}}} \frac{\cos\beta}{\sin i} sin\theta_0 + \lambda_i \frac{\cancel{2A\sqrt{a}}}{\cancel{\pi\sqrt{\mu}}} \cos\beta \, cos\theta_0$$

$$= -\pi\lambda_a a \sin\beta + \lambda_\Omega \frac{\cos\beta}{\sin i} sin\theta_0 + \lambda_i \cos\beta \, cos\theta_0 = 0 \qquad (3.36)$$

Hence,

$$\tan\beta = \frac{\Lambda}{\lambda_a \pi a} \qquad (3.37)$$

and

$$\sin\beta = \frac{\Lambda}{\sqrt{\Lambda^2 + (\lambda_a \pi a)^2}} \qquad (3.38)$$

$$\cos\beta = \frac{\lambda_a \pi a}{\Lambda^2 + (\lambda_a \pi a)^2} \qquad (3.39)$$

At this point, observing these results some considerations need to be done:

- From Eq. 3.31 we see that $cos\,\beta$ must be concordant with λ_a to guarantee the maximization of the Hamiltonian. Therefore λ_a tells us how to perform the manoeuvre: if it is positive we need to increase the Semimajor axis because β would be positive: if it is negative, β is also negative and we would need to decrease the Semimajor axis;

- $\sin\beta$ needs to be concordant with $\left(\frac{\lambda_\Omega sin\theta_0}{\sin i} + \lambda_i cos\theta_0\right)$ and this means that $sin\theta_0$ and $cos\theta_0$ need to be concordant with $\frac{\lambda_\Omega}{\sin i}$ and λ_i respectively;

- Eq. 3.34 and Eq. 3.37 are the main equations of our problem since they give the optimum values of our control. The next step has been to compile a MATLAB script able to solve the system of five ordinary differential equations (ODEs) expressed by Eq. 3.30 and Eq. 3.32 ($\lambda_\Omega = 0$ is obviously neglected). This step is developed in the next paragraph.

3.1.3 Solution of the BVP

Eq. 3.30 and 3.32 constitute our BVP, summarised in Eq. 3.40, and a Genetic Algorithm needs to be implemented to solve it.

$$\frac{da}{dt} = \frac{2A}{\sqrt{\mu}} a^{\frac{3}{2}} \cos\beta$$

$$\frac{d\Omega}{dt} = \frac{2A\sqrt{a}}{\pi\sqrt{\mu}} \frac{\sin\beta}{\sin i} sin\theta_0 - \frac{3}{2} j_2 \frac{R_e^2}{a^{\frac{7}{2}}} \cos i \ \sqrt{\mu}$$

$$\frac{di}{dt} = \frac{2A\sqrt{a}}{\pi\sqrt{\mu}} \sin\beta \, cos\theta_0 \tag{3.40}$$

$$\dot{\lambda_a} = -\left[\lambda_a \frac{3A}{\sqrt{\mu}} \sqrt{a} \cos\beta + \lambda_\Omega \left(\frac{A}{\pi\sqrt{\mu}} \frac{\sin\beta}{\sin i} \ \frac{sin\theta_0}{\sqrt{a}} \ - \frac{21}{4} j_2 \frac{R_e^2}{a^{\frac{9}{2}}} \cos i \ \sqrt{\mu} \right) + \lambda_i \left(\frac{A}{\pi\sqrt{\mu}} \ \frac{1}{\sqrt{a}} \sin\beta \, cos\theta_0 \right) \right]$$

$$\dot{\lambda_1} = -\lambda_\Omega \left(-\frac{2A\sqrt{a}}{\pi\sqrt{\mu}} \frac{\sin\beta}{\sin^2 i} \cos i \, sin\theta_0 + \frac{3}{2} j_2 \frac{R_e^2}{a^{\frac{7}{2}}} \sin i \ \sqrt{\mu} \right)$$

Our Boundary Value Problem
(State Equations)

Eq. 3.34 and 3.37 represent the control equations that a potential solution of the BVP must satisfy to become a possible optimum value.

The control equations are summarised in Eq. 3.41

$$\tan\theta_0 = \frac{\lambda_\Omega}{\lambda_\mathrm{i}\sin i} \tag{3.41a}$$

$$\tan\beta = \frac{\Lambda}{\lambda_a \pi a} \tag{3.41b}$$

Following this very analytical and manual part of our study, during which only a pen and a lot of papers have been used, we had finally the possibility to benefit from today's technological progress and use a calculator to solve the BVP and show the final results.

Mathworks' MATLAB has been used to perform the optimisation and to solve the 5-ODEs system constituting the BVP, using both a Genetic Algorithm and ***fminsearch*** to guarantee the convergence towards the global optimum (minimum in this case). We will give a very fast overview of the way we proceeded.

The path we travelled through is here analysed very simply, since our goal is to make even an aerospace-unfamiliar reader able to follow the crux of the matter.

In the first part we had to define the inputs of the problem, already mentioned in the previous chapters. We have set three different types of parameters:

- The S/C characteristics, such as mass, specific impulse and thrust, and the lowest altitude that the S/C is allowed to reach;
- The initial conditions of the S/C's orbit like altitude, inclination and RAAN;

- The desired variation in altitude, inclination and RAAN in order to reach the final orbit (here, obviously, the values may be either positive or negative);

Following the input part, the normalisation of each variable has been performed to simplify the calculation process; immediately after, it has been necessary to define the function that the genetic algorithm had to use to find the global optimum: in our case, the function has been named "errore" and it is expressed by

$$errore = \sqrt{\left(\bar{a} - a_f\right)^2 + \left(\bar{\imath} - i_f\right)^2 + \left(\bar{\Omega} - \Omega_f\right)^2} \tag{3.42}$$

where $\bar{a}, \bar{\imath}, \bar{\Omega}$ are the solutions of the GA while a_f, i_f, Ω_f are the target solutions, determined as sum of the initial value and the desired variation.

The GA have received from the inputs the function "errore", the number of variables – in our case the variables are three i.e. the final time t_f and the initial values of λ_a and λ_i – and the range of values that the variables can have. We have then set a wide range of values, since we needed to be sure to find the global optimum. The GA has given random values to the three variables, it has determined the control parameters β and θ_0 and calculated the value of the function, giving the set of random estimations a fitness value. Once the stopping criteria has been fulfilled, it has stopped and given the values of t_f, λ_a, λ_i that minimise the function and the final solutions $\bar{a}, \bar{\imath}, \bar{\Omega}$.

At this point, a check had to be performed, considering that, for certain missions, the minimum altitude may have been reached and passed: in this case, the solution

would not be acceptable. If, instead, the minimum altitude is not passed, the solution is correct and can be given as input to ***fminsearch***.

Considering the first possibility, we needed to perform a more accurate simulation of the problem. In this case we needed to split the manoeuvre into three parts:

- the first one starts from the initial point (t_0) and ends when the S/C reaches the minimum altitude (t_1);
- the third consists of the time needed to reach the final conditions at the final time from the minimum altitude ($t_2 \div t_f$);
- the second represents the variable section, since it depends on the other two and the total mission time ($t_1 \div t_2$);

Therefore, the number of variables has increased to five ($t_1, t_2, t_f, \lambda_a, \lambda_i$), since also the integration needed to be split:

$$\int_{t_0}^{t_f} \frac{dx}{dt} = \int_{t_0}^{t_1} \frac{dx}{dt} + \int_{t_1}^{t_2} \frac{\widetilde{dx}}{dt} + \int_{t_2}^{t_f} \frac{dx}{dt} \tag{3.43}$$

The peculiarity of this problem is that during the second part, the Semimajor axis must remain constant as well as λ_a: this means that Eq. 3.40 needs to be modified to a new version $\frac{\widetilde{dx}}{dt}$, since the first and the fourth equation must be set equal to zero and β equal to 90 deg (in fact only with this value, a remains constant).

Once the GA ended to run, as the other case, it has given the vector of the solutions which may represent the global optimum. However, we needed to make sure that

the values were the real optima, otherwise ***fminsearch*** shall find them out. As explained in paragraph 2.6, in order to be able to find the correct global optimum, ***fminsearch*** needs a quite accurate initial value, especially if a multi-variable problem is considered. Therefore, we decided to provide the GA's solutions as input: since GA finds out a moderately accurate solution, we could be sure that it will calculate in output the global optimum.

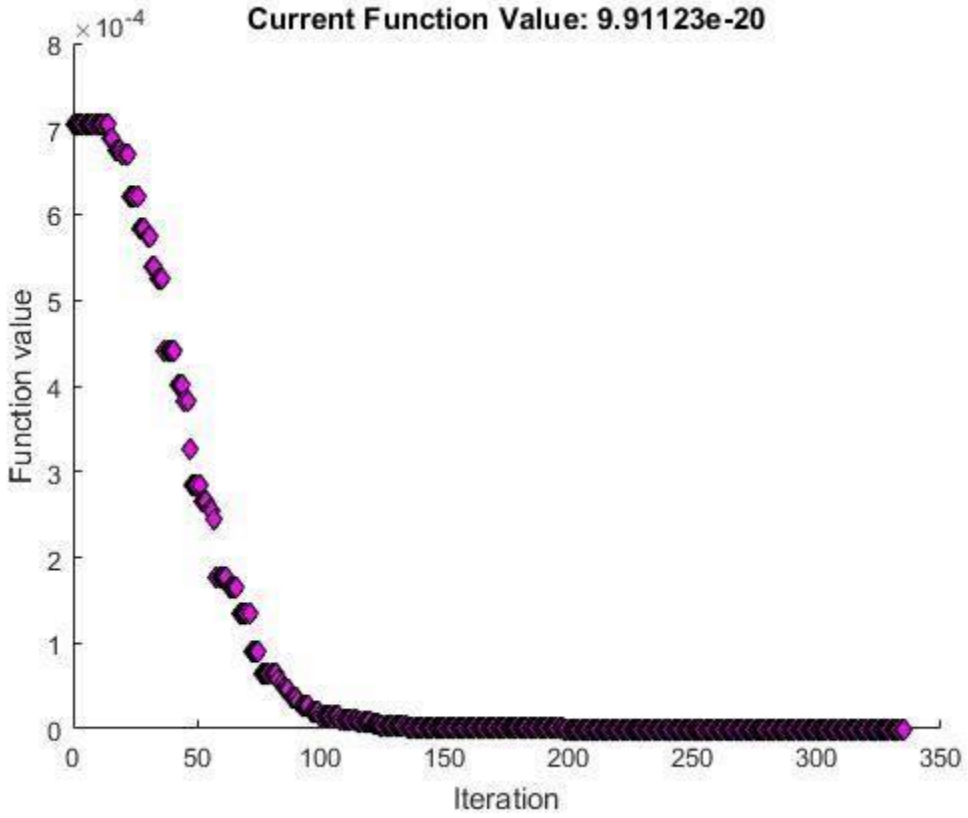

Figure 17: Convergence of fminsearch

In fact, Figure 17 shows the convergence of ***fminsearch*** which brings the value of the function "errore" to be in the order of $10^{-17}/10^{-20}$.

The output of the analysis consists of the values of the vector $x = [t_1, t_2, t_f, \lambda_a, \lambda_i]$ – times are in days to better understand the duration of the manoeuvre - and the evolution in time of the five parameters $a,\ i,\ \Omega,\ \lambda_{\mathrm{a}},\ \lambda_{\mathrm{i}}$.

The goal of this study, however, is to present an overview of the cost of the studied manoeuvre in terms of ΔV and mass of propellant (m_p). Therefore, we need to calculate these parameters.

To do that, two simple formulations are used:

$$\Delta V = \frac{T}{m_0} \cdot t_f \tag{3.44}$$

$$m_p = m_0 \left(1 - e^{-\frac{\Delta V}{c}}\right)$$

where the second one is the famous Tsiolkovsky rocket equation [1], m_0 is the initial mass, T is the S/C's thrust and c is the effective exhaust velocity.

After this brief overview about the steps followed for the optimisation, we are now ready to present the results of a default simulation and, successively, the estimation for other different simulations, realised by changing some parameters from the default one.

[1] TSIOLKOWSKY K, *Esplorazione degli spazî cosmici con razzi a propulsione*, 1903

3.2 The Analyses

In this paragraph the results of two simulations made for the scenario presented in Chapter 1, and shown in Figure 7, are presented: one has a positive change in RAAN (+30°) whereas the second has a negative one (-30°).

3.2.1 Positive ΔΩ

The first case consists of a positive change in altitude and RAAN, without varying the inclination. As mentioned in Chapter 1, these are the inputs:

$$\begin{aligned} a_0 &= 500\ Km & \Delta a &= 100\ Km \\ i_0 &= 0° & \Delta i &= 0° \\ \Omega_0 &= 0° & \Delta\Omega &= +30° \end{aligned} \tag{3.45}$$

This case is the simplest of the two presented in this paragraph, since it does not entail the reaching of the minimum altitude: in fact, as shown later in Figure 18, the manoeuvre will first consist of an increase in altitude and then a decrease. Different behaviour will have the second case.

The results of this first analysis gives:

$$\begin{aligned} \Delta V &= 1{,}3869\ Km/s \\ m_p &= 0{,}8247\ Kg \\ t_f &= 24{,}07\ days \\ \lambda_a &= 2{,}6359 \\ \lambda_i &= 0{,}9212 \end{aligned} \tag{3.46}$$

These values are specific for the particular set of inputs shown in Eq. 3.45; however, in paragraph 3.3 it is possible to verify that these values can give a good overview of other scenarios since results will not be so far from them.

We believe that it may be useful to show the evolution of the five parameters $a,\ i,\ \Omega,\ \lambda_a,\ \lambda_i$ because it offers a simple and easily understandable method to explain how the transfer occurs.

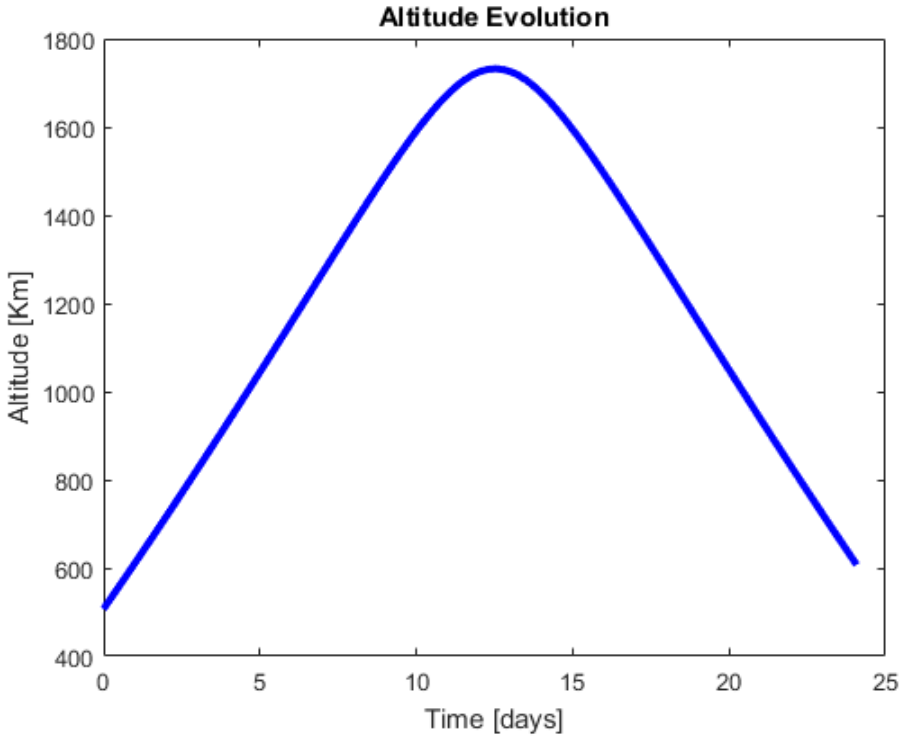

Figure 18: Evolution of Altitude with time (Case $\Delta\Omega^+$)

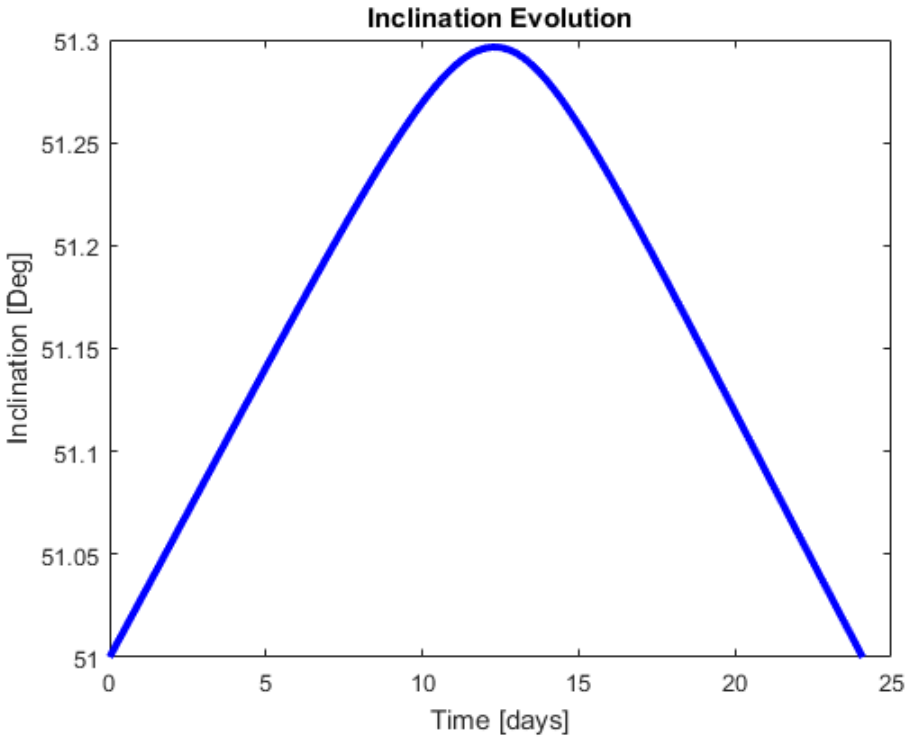

Figure 19: Evolution of Inclination with time (Case $\Delta\Omega^+$)

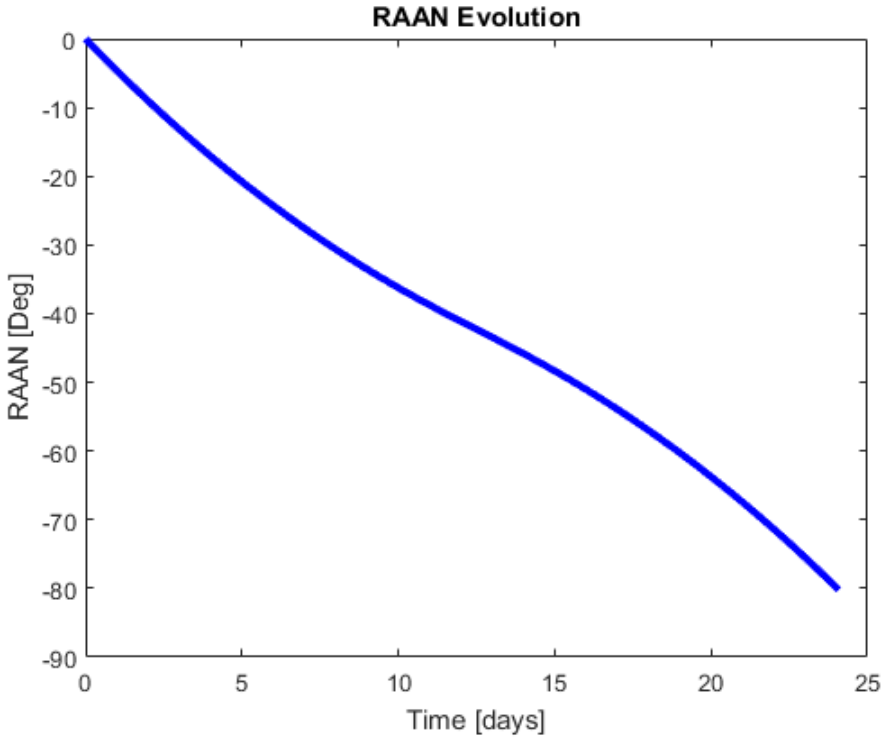

Figure 20: Evolution of RAAN with time (Case $\Delta\Omega^+$)

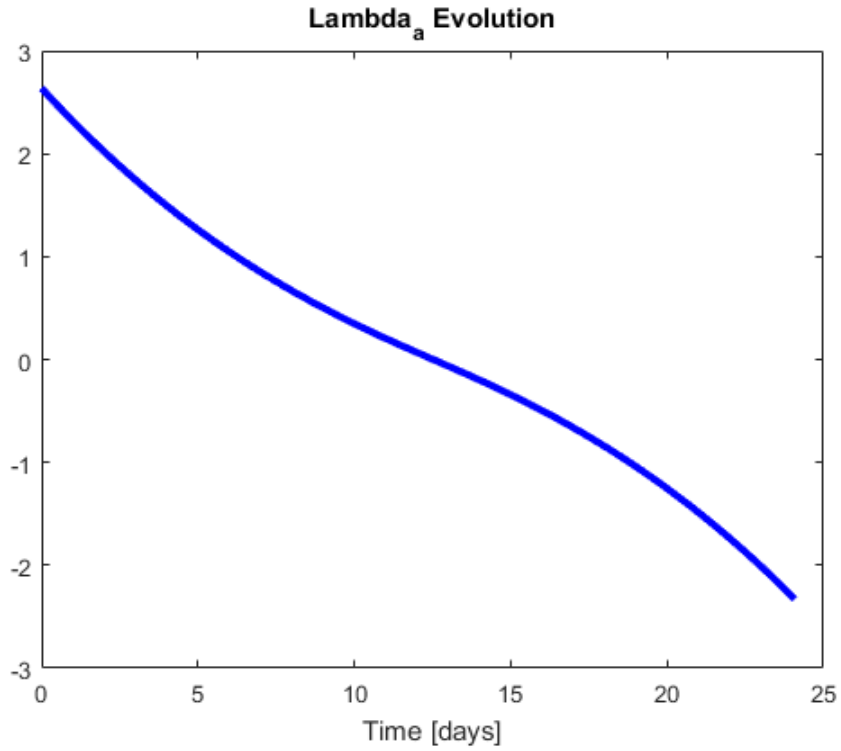

Figure 21: Evolution of λ_a with time (Case $\Delta\Omega^+$)

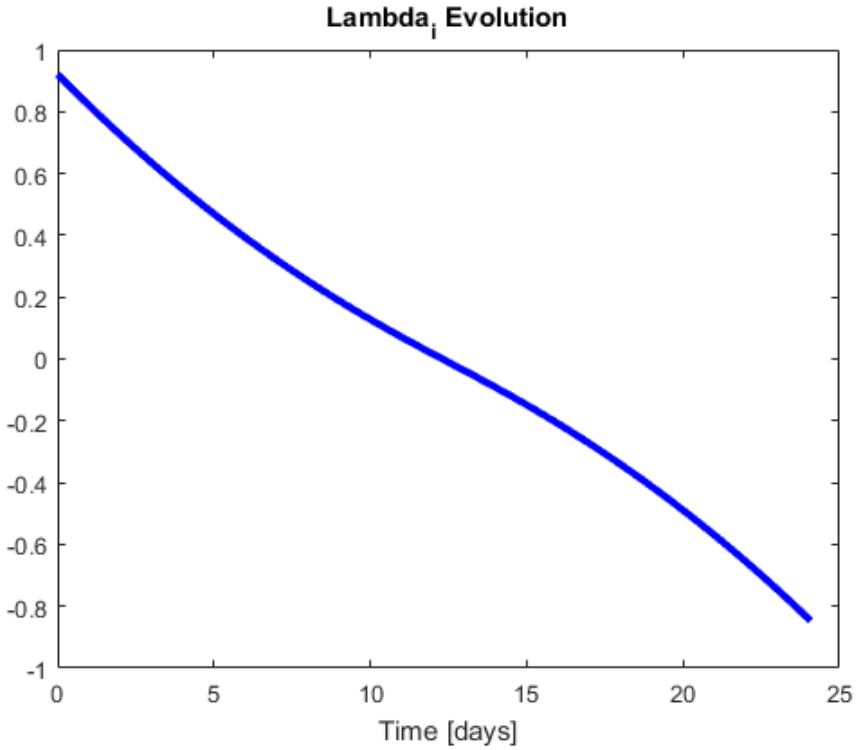

Figure 22: Evolution of λ_i with time (Case $\Delta\Omega^+$)

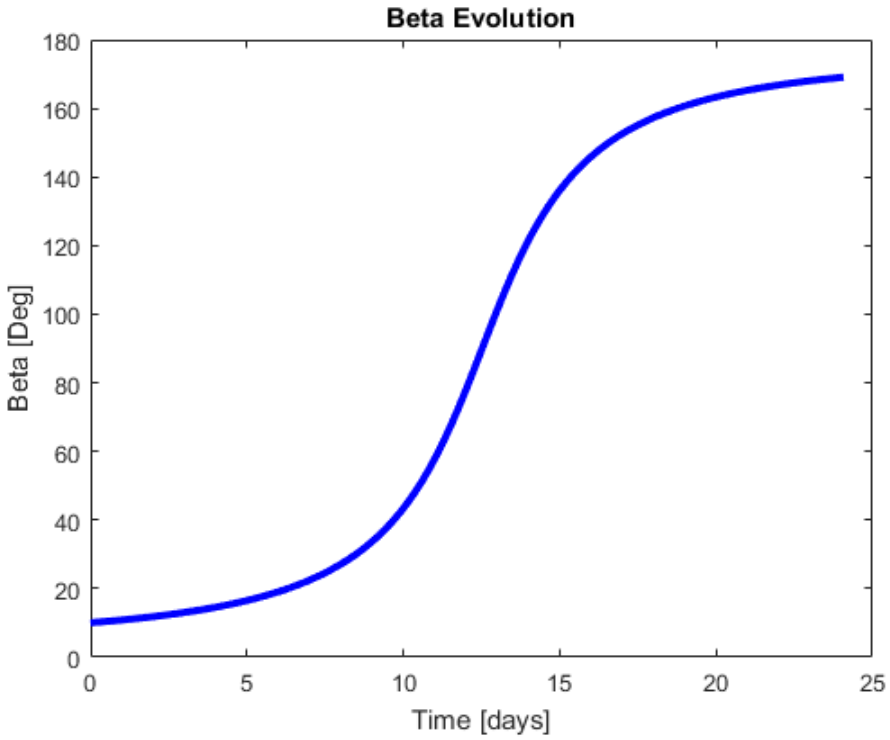

Figure 23: Evolution of β with time (Case $\Delta\Omega^+$)

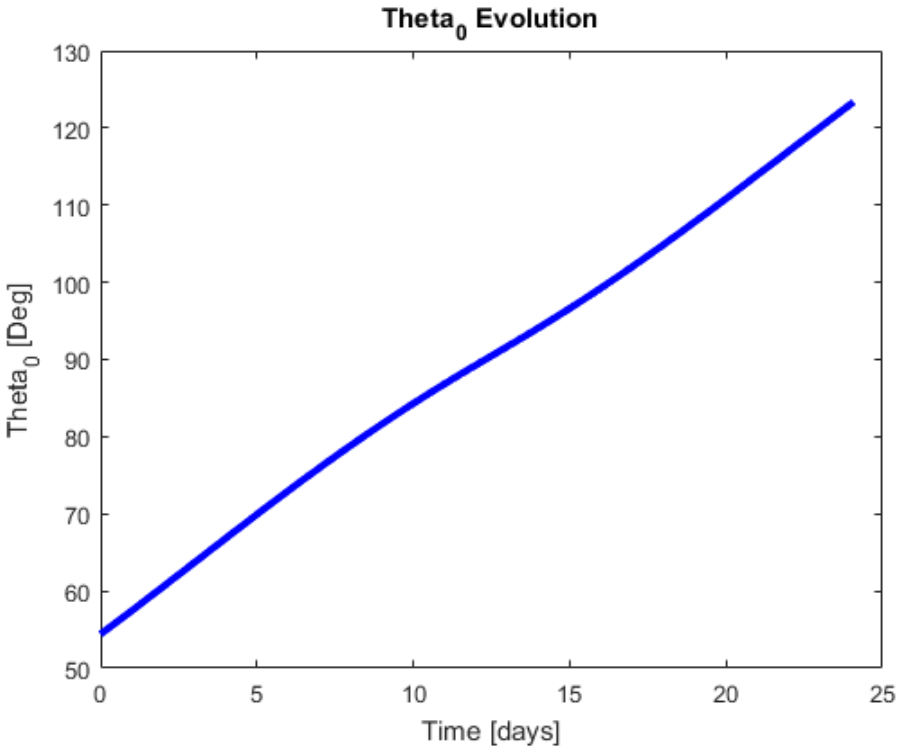

Figure 24: Evolution of θ_0 with time (Case $\Delta\Omega^+$)

The first three figures show the evolutions of the three Keplerian elements. It is easy to understand that the manoeuvre consists of a continuous and combined variation of them: altitude and inclination are first increased and then decreased until reaching the target, whereas the RAAN decreases only. This behaviour is the key of our study: the S/C increases the altitude in order to take advantage of the j_2 effect which, as we observed, has a greater influence the greater is the altitude difference. This approach guarantees a considerable benefit in terms of time and propellant; in fact, two other options would be possible: staying on the same orbit, waiting for j_2 to nullify the $\Delta\Omega$ and align the two planes – and this would take years and years although fuel consumption would be nearly paltry – or to still remain on the same orbit but directly rotate the orbital plane – which would have an enormous fuel cost. It is also clear that, with an appropriate timing choice, the S/C would reach the final orbit in a specific point of it, which could be for example the catching distance of a robotic arms belonging to one of the platforms presented in Chapter 1.

It is important to note that, unlike for altitude and inclination, the final value of the RAAN in Figure 20 is not the real final one: in fact, we expect a value of 30° but we obtain -80,227°. This is due to the fact that this graph does not consider the effect of j_2 on RAAN evolution with time. To find the final value, it is necessary to sum that value and the $\dot{\Omega} \cdot t_f$ obtained by substituting the solutions $a_f,\ i_f,\ \Omega_{\mathrm{f}},\ \lambda_{\mathrm{a}_f},\ \lambda_{\mathrm{i}_f}$ in the second of Eq. 3.40. In fact, for the final value, we find:

$$\dot{\Omega} = \ -7{,}4608\ 10^{-4}\ rad/\bar{T}$$

$$\dot{\Omega} \cdot t_f = -1{,}9239\, rad = -110{,}23\, deg$$

$$\Omega_f = 30{,}01\, deg$$

where $\bar{T}$ is a normalised time.

Figures 21 and 22 show the evolution of λ_a and λ_i: both start from a positive value and end with a negative one, passing the zero almost in the same moment: we will see that this behaviour will not occur with a negative $\Delta\Omega$. Figures 23 and 24 show the evolution of the control variables β and θ_0. Like the previous parameters, also in these two we find a symmetry. The first presents a variation that starts very slightly and increases with time until the maximum reached, as predicted, at the half of the entire duration when β is worth 90 deg. It starts from a value lower than 90 deg since the component of the acceleration needs to be concordant with the velocity: the altitude needs to increase. From that point, the slope starts decreasing again but the value of β keeps increasing: passing 90 deg, the acceleration is now discordant with the velocity since S/C needs to break and to decrease the orbit altitude to reach the target. θ_0 has a quite different behaviour, since its slope remains nearly constant and positive during the whole duration. With these two control variables, it is possible to obtain the three components of the acceleration as function of time: these parameters will be given as input to the S/C's navigation system and will be the key to perform the fulfilment of the transfer.

3.2.2 Negative ΔΩ

This second simulation has been made with the following inputs:

$$a_0 = 500\ Km \qquad \Delta a = 100\ Km$$
$$i_0 = 0° \qquad \Delta i = 0°$$
$$\Omega_0 = 0° \qquad \Delta\Omega = -30°$$

In this case we will see the S/C reaching the minimum altitude. Therefore, as explained previously, the manoeuvre will be accomplished through three steps.

The results of the analysis give:

$$\Delta V = 1{,}4009 \frac{Km}{s}$$

$$m_p = 0{,}8328\ Kg$$

$$t_f = 24{,}32\ days$$

$$\lambda_a = -1{,}2763$$

$$\lambda_i = 1{,}4390$$

We can take a look to the evolution of the five parameters and notice a great difference with respect to the previous case.

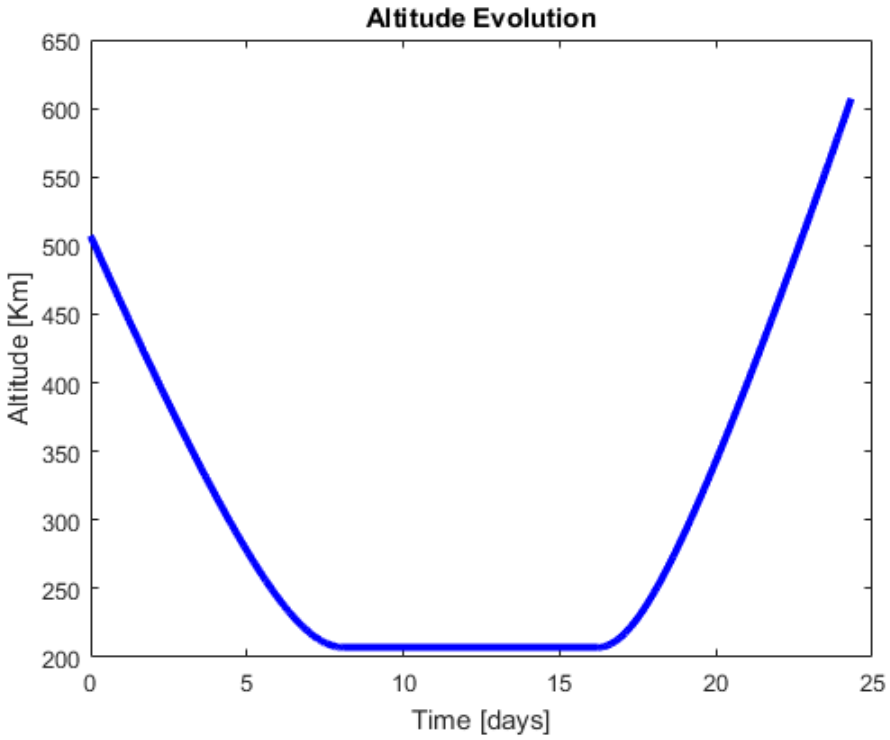

Figure 25: Evolution of Altitude with time (Case $\Delta\Omega^-$)

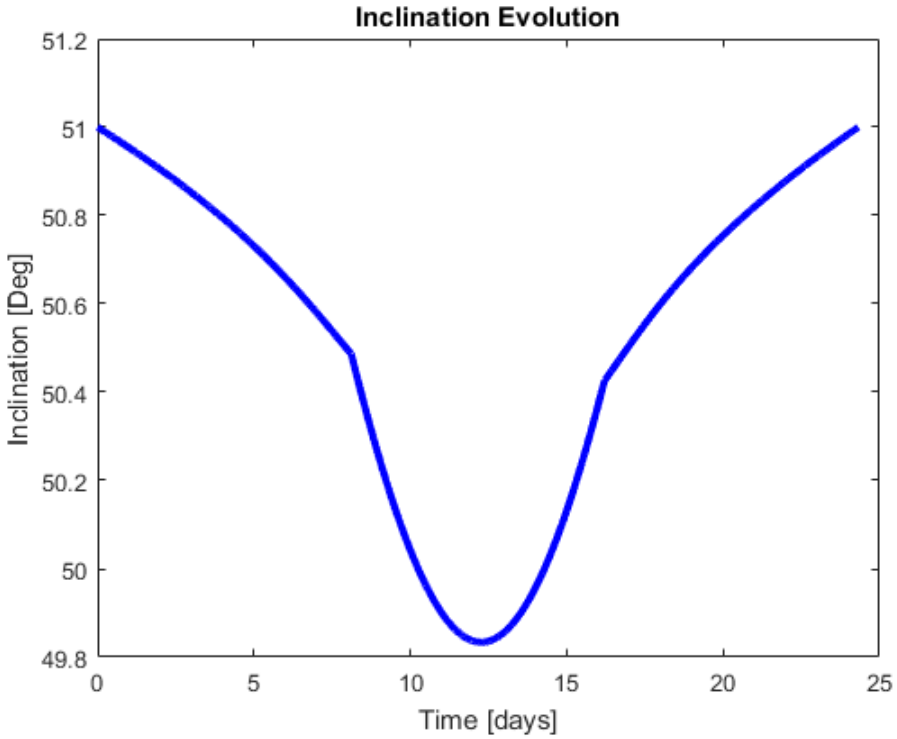

Figure 26: Evolution of Inclination with time (Case $\Delta\Omega^-$)

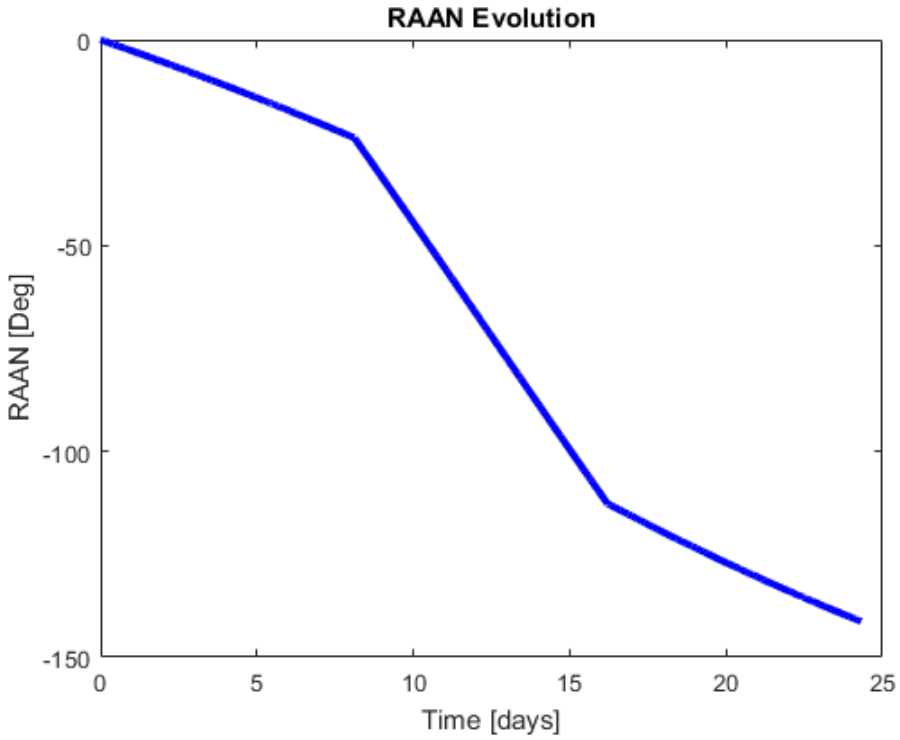

Figure 27: Evolution of RAAN with time (Case $\Delta\Omega^-$)

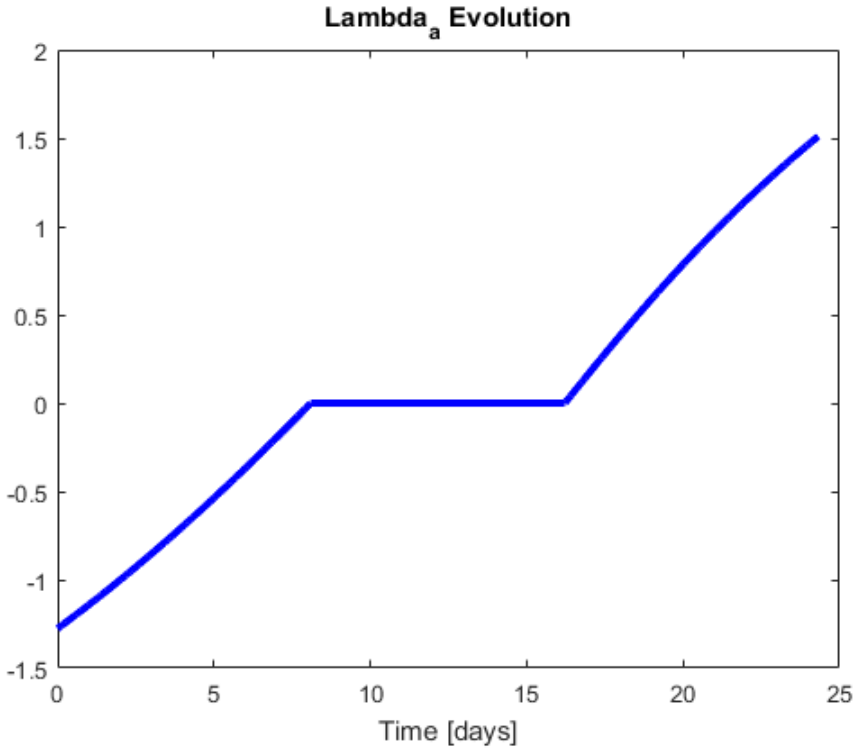

Figure 28: Evolution of λ_a with time (Case $\Delta\Omega^-$)

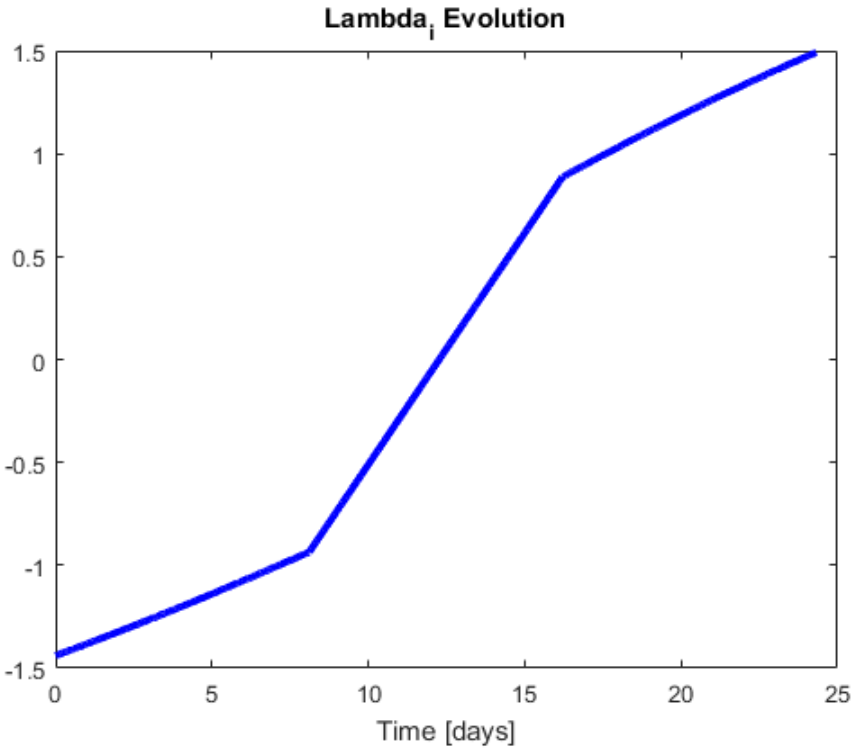

Figure 29: Evolution of λ_i with time (Case $\Delta\Omega^-$)

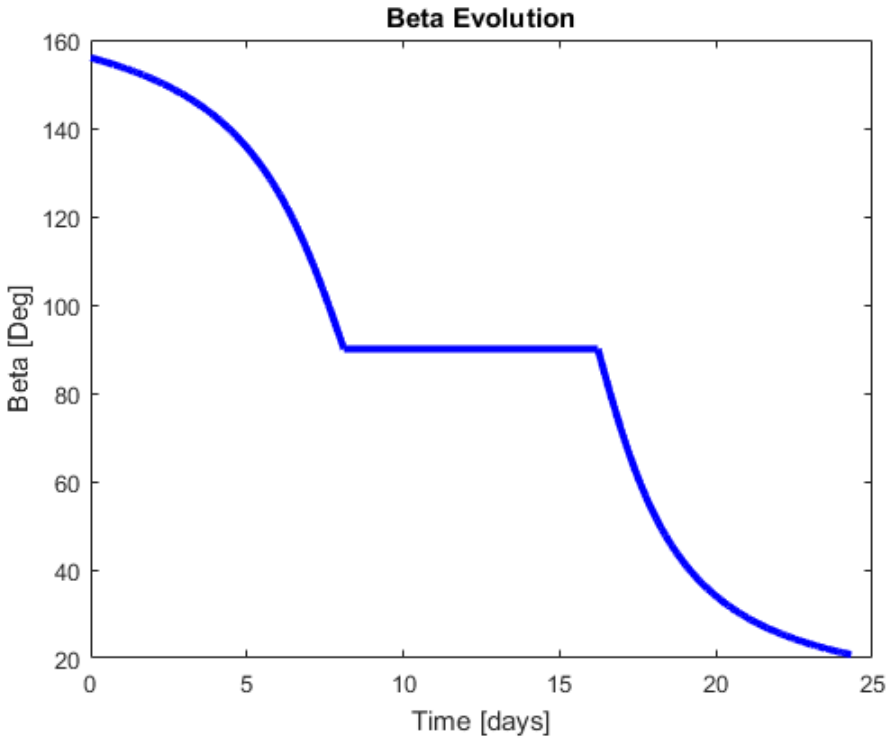

Figure 30: Evolution of β with time (Case $\Delta\Omega^-$)

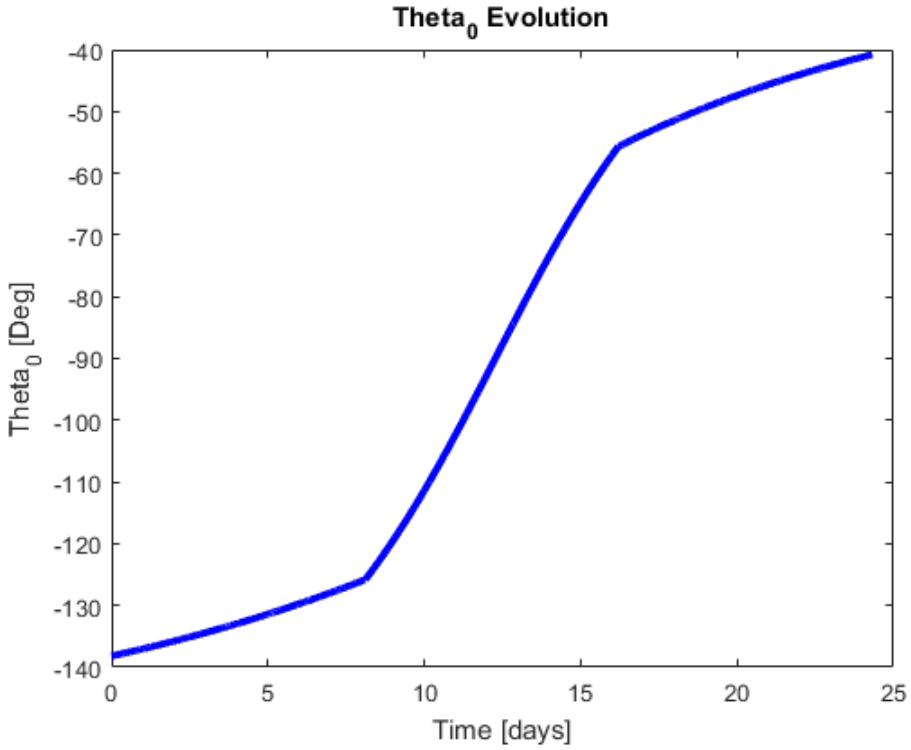

Figure 31: Evolution of θ_0 with time (Case $\Delta\Omega^-$)

First thing that stands out is the opposite evolution of each parameter except for RAAN: altitude and inclination decrease first and then increase, while λ_a and λ_i have a positive slope.

The second important finding is the particular shape of each graph: they have lost the simple linearity of the first case. This is due to the split of the integral: in each figure it is possible to identify three different sections of the curve: the first and the second have mostly the same (Figures 27,28,29) or symmetric (Figure 25 and 26) attitude while the second shows an abrupt change.

Figure 25 shows that the S/C descends until it reaches the minimum altitude: during this manoeuvre, the inclination also decreases (Figure 26) as well as the RAAN (Figure 27).

Once the S/C reaches the minimum altitude, it needs to stop descending and this is why both Figures 25 and 28 show a plateau: during the second part, in fact, the altitude remains constant while inclination and RAAN decrease with a slope clearly greater than before. This is also due to the j_2 effect, which increases the velocity of the process. During the third part, the S/C has a symmetric behaviour to the one in the first part, and this is why the slopes are so similar: obviously, RAAN keeps decreasing, even with a lower intensity, whereas altitude and inclination tend to increase again to reach the final values. As shown in Figure 30, β starts from a value higher than 90 deg - which means that the component of the acceleration is slowing down the S/C (i.e. it is opposite to the S/C velocity) - and this causes the altitude to decrease. Reaching the minimum altitude, the S/C must not change the altitude anymore and this is why β remains constant on the value of 90 deg. Once the spacecraft has completed the second part of the manoeuvre, β starts decreasing again but with an acceleration that this time is concordant with the velocity: this cause the S/C to accelerate and the altitude to increase again.

These two cases mostly summarise all the possible solutions: obviously, with different parameters, the results will be different, but the manoeuvre will be performed in one of the two ways already shown. In the next paragraph the results of many other simulations are presented: due to a limited number of pages (and limited time), it is not possible to analyse in detail every case, therefore the results will be given only in terms of $\Delta V, m_p, t_f, \lambda_a, \lambda_i$.

3.3 Other Examples of Simulations

Different simulations have been performed, gradually changing first the desired $\Delta\Omega$ and then the desired Δa (keeping the other default settings); in the end, only one simulation has been made with a different value of thrust, specific impulse and mass in order to provide an estimation of the influence of the thrust on the results.

3.3.1 Changing in ΔΩ

A range of $[-70; 70]$ is here considered with a mass of $15\ Kg$, a thrust of $0{,}01\ N$, altitude difference of $100\ Km$ and inclination difference of $0\ deg$.

$\Delta a = 100\ Km, \Delta i = 0\ deg, m_0 = 15\ Kg, Thrust = 0{,}01\ N$					
ΔΩ	**$\Delta V\ [Km/s]$**	**$m_p\ [Kg]$**	**$t_f\ [days]$**	**λ_a**	**λ_i**
-70	2,7567	1,5948	47,8596	-1,4770	-2,8322
-60	2,4410	1,4210	42,3776	-1,4303	-2,5149
-50	2,1108	1,2370	36,6467	-1,3807	-2,1785
-40	1,7647	1,0414	30,6369	-1,3288	-1,8207
-30	1,4009	0,8328	24,3206	-1,2763	-1,4390
-20	1,0186	0,6102	17,6843	-1,2279	-1,0320
-10	0,6196	0,3742	10,7573	-1,1931	-0,6038
0	0,0580	0,0354	1,0066	1,2360	0,0525
10	0,7624	0,4591	13,2359	1,6869	0,5879
20	1,1111	0,6644	19,2901	2,2468	0,7870
30	1,3869	0,8247	24,0782	2,6359	0,9212
40	1,6260	0,9622	28,2292	2,9386	1,0231
50	1,8421	1,0854	31,9813	3,1869	1,1047
60	2,0422	1,1985	35,4552	3,3972	1,1722
70	2,2304	1,3039	38,7217	3,5791	1,2293

Table 4: Results changing the ΔΩ

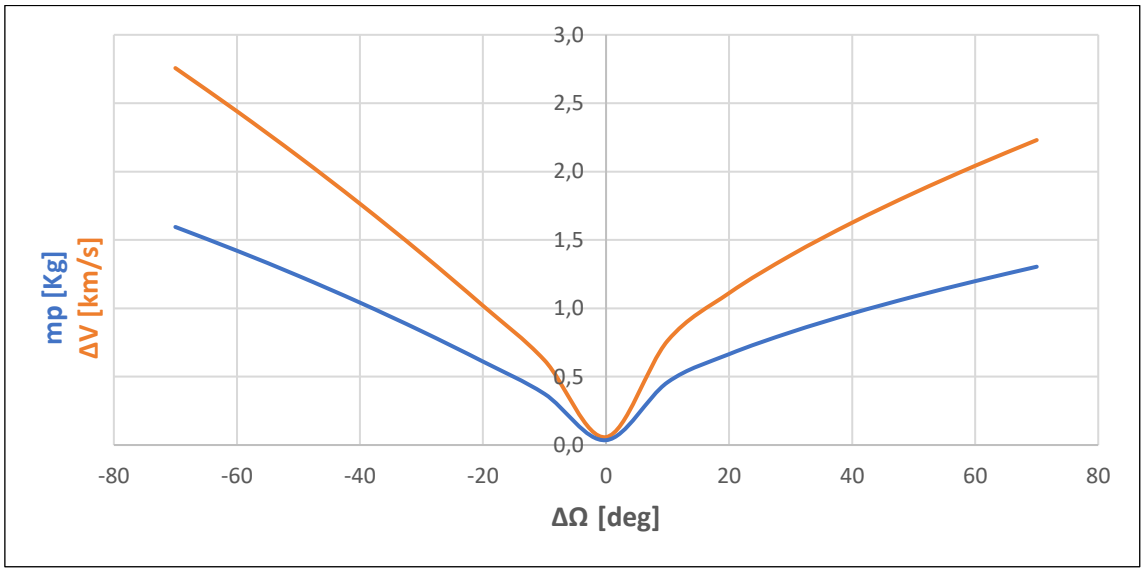

Figure 32: Evolution of the costs with ΔΩ

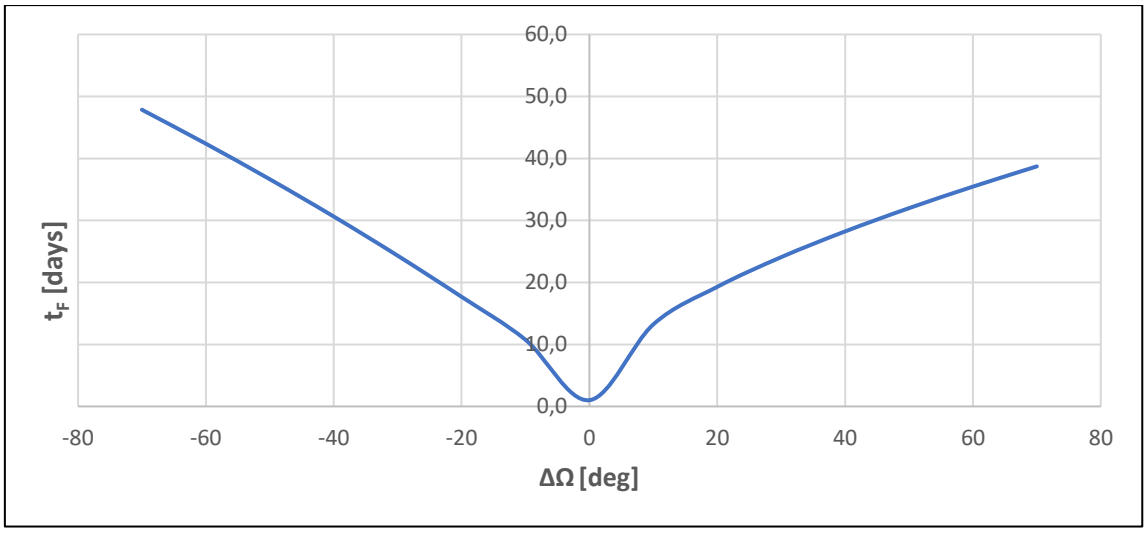

Figure 33: Evolution of transfer duration with ΔΩ

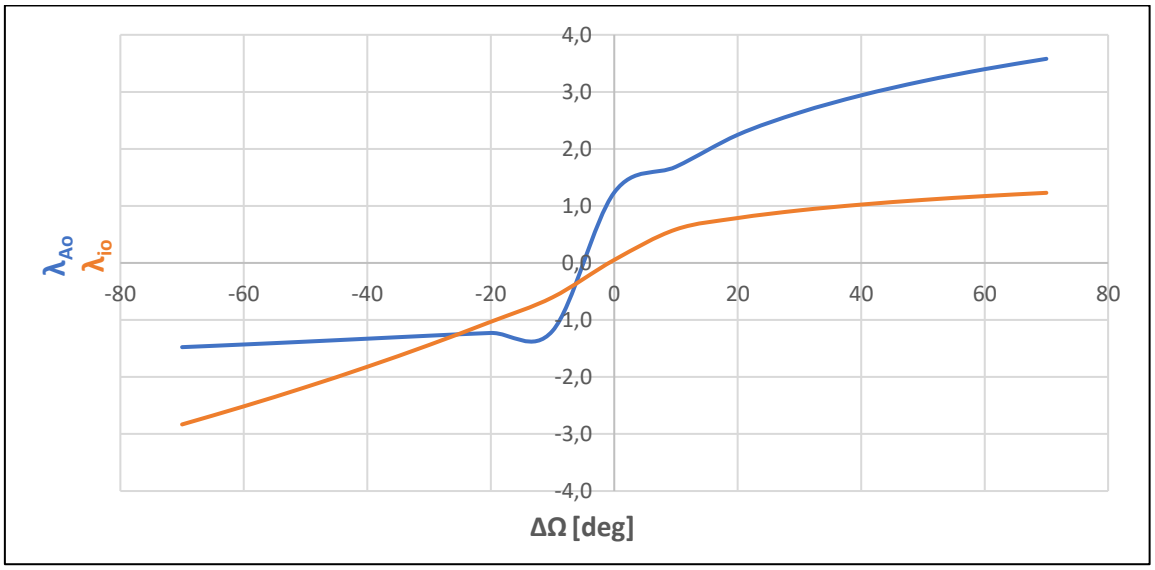

Figure 34: Evolution of λ_a and λ_i with $\Delta\Omega$

This first set of graphs show an antisymmetric behaviour of the parameters between positive and negative desired $\Delta\Omega$; this is due to the j_2 effect which has more benefits with positive $\Delta\Omega$ proved by a lower value of $\Delta V, m_p$ *and* t_f considering same absolute value of $\Delta\Omega$. Obviously, the antisymmetric behaviour affects also λ_a and λ_i.

3.3.2 Changing in Δa

Regarding the change of Δa, we would like to show the evolution of the costs and the influence of the target distance, intended as altitude distance. Here is considered a minimum altitude difference of $100\ km$ and a maximum of $2000\ Km$. It is possible to notice an obvious remarkable increase in propulsive and time costs (Table 5).

$\Delta\Omega = 30\ deg, \Delta i = 0\ deg, m_0 = 15\ Kg, Thrust = 0,01\ N$					
Δa	**$\Delta V\ [Km/s]$**	**$m_p\ [Kg]$**	**$t_f\ [days]$**	**λ_a**	**λ_i**
100	1,3869	0,8247	24,0782	2,6359	0,9212
200	1,4764	0,8763	25,6312	2,8215	0,9731
300	1,5697	0,9300	27,2523	2,9993	1,0230
400	1,6666	0,9855	28,9345	3,1691	1,0708
500	1,7667	1,0425	30,6713	3,3305	1,1163
600	1,8695	1,1009	32,4567	3,4834	1,1593
700	1,9748	1,1605	34,2850	3,6280	1,1997
800	2,0823	1,2210	36,1511	3,7642	1,2375
900	2,1917	1,2823	38,0505	3,8924	1,2727
1000	2,3028	1,3443	39,9791	4,0126	1,3054
1100	2,4154	1,4069	41,9332	4,1252	1,3356
1200	2,5292	1,4698	43,9094	4,2307	1,3633
1300	2,6441	1,5331	45,9050	4,3292	1,3887
1400	2,7600	1,5966	47,9171	4,4212	1,4119
1500	2,8767	1,6602	49,9436	4,5070	1,4329
1600	2,9942	1,7239	51,9821	4,5871	1,4520
1700	3,1122	1,7876	54,0307	4,6618	1,4691
1800	3,2306	1,8513	56,0876	4,7314	1,4844
1900	3,3495	1,9149	58,1511	4,7962	1,4981
2000	3,4686	1,9783	60,2196	4,8567	1,5101

Table 5: Results changing the Δa

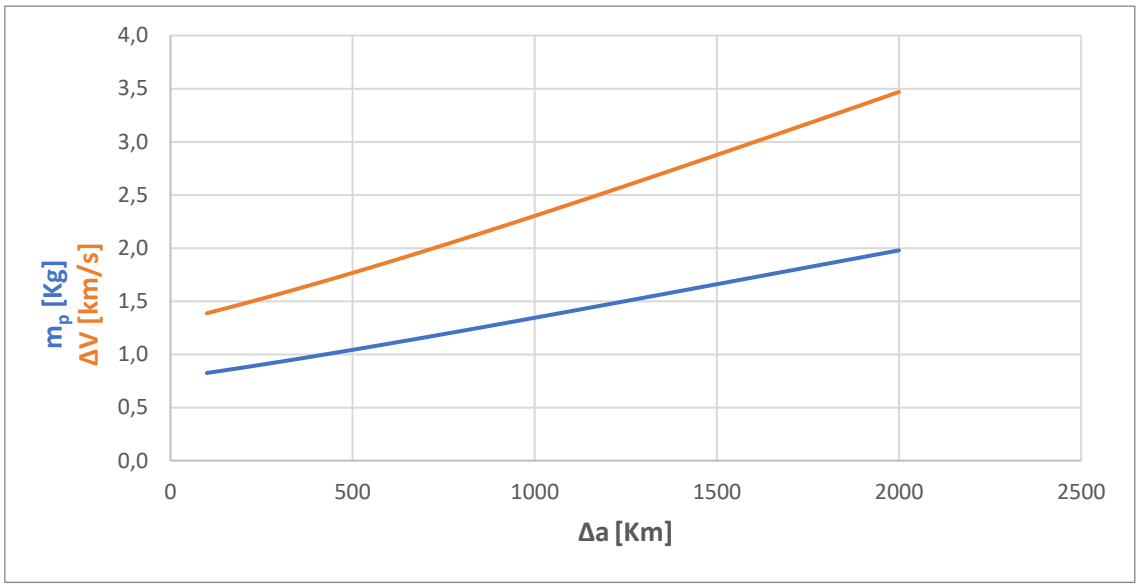

*Figure 35: Evolution of the costs with **Δa***

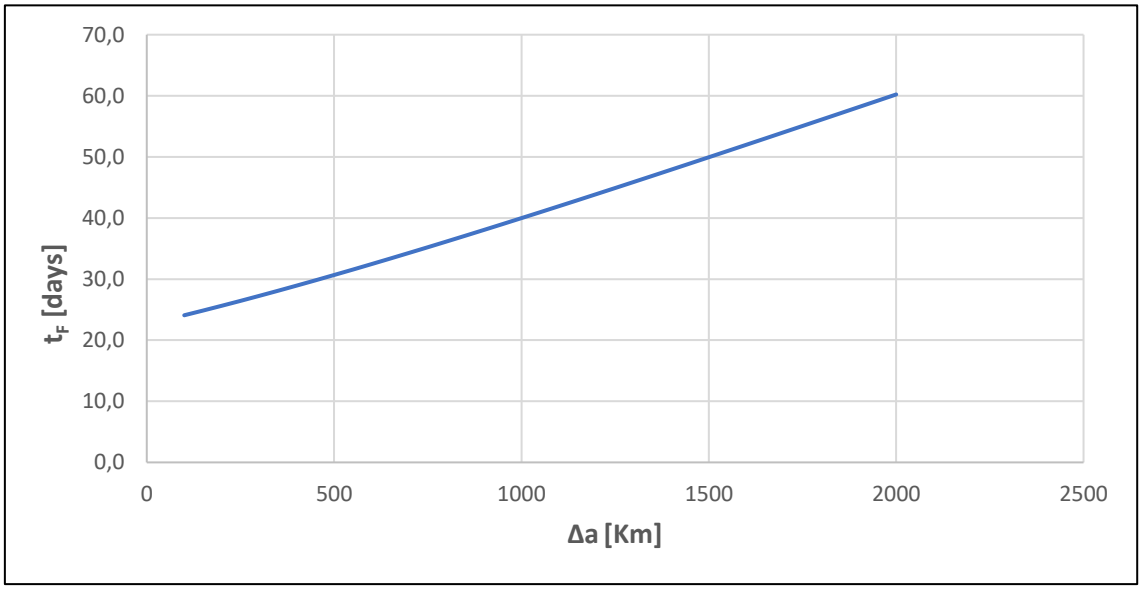

*Figure 36: Evolution of transfer duration with **Δa***

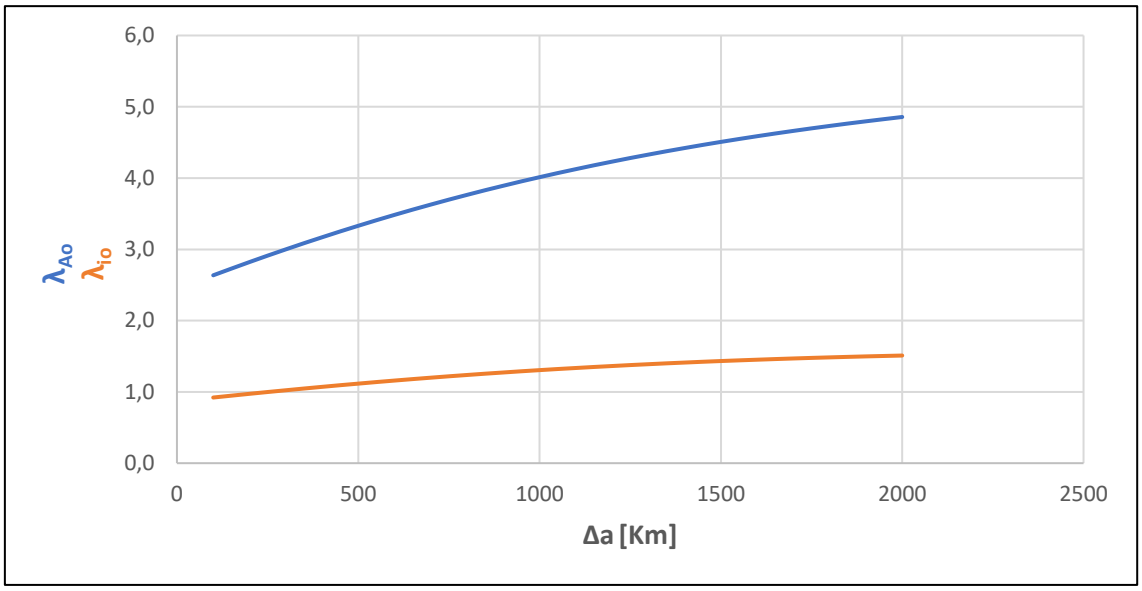

Figure 37: Evolution of λ_{a_0} and λ_{i_0} with Δa

3.3.3 Changing in Thrust, ISP and Mass

In this final paragraph we would like to show the influence of a change in specific impulse, thrust and mass. We have considered the default case of the paragraph 3.3.2. Tables 6, 7 and 8 show the difference between the results by changing each parameter.

	$I_{sp} = 2500$ s	$I_{sp} = 3500\ s$
ΔV	$1{,}4009\frac{Km}{s}$	$1{,}4009\frac{Km}{s}$
m_p	$0{,}8328\ Kg$	$0.5997\ Kg$
t_f	$24{,}32\ days$	$24.32\ days$

Table 6: Influence of changing Isp

	$T = 0{,}01\ N$	$T = 0{,}02\ N$
ΔV	$1{,}4009\frac{Km}{s}$	$2{,}1040\frac{Km}{s}$
m_p	$0{,}8328\ Kg$	$1{,}2332\ Kg$
t_f	$24{,}32\ days$	$18{,}26\ days$

Table 7: Influence of changing the initial Thrust

	$m_o = 15\ Kg$	$m_0 = 30\ Kg$
ΔV	$1{,}4009\frac{Km}{s}$	$0{,}8934\frac{Km}{s}$
m_p	$0{,}8328\ Kg$	$1{,}0732\ Kg$
t_f	$24{,}32\ days$	$31{,}02\ days$

Table 8: Influence of changing the initial Mass

As predictable, the I_{SP} has a relevant influence in the fuel consumption whereas ΔV and transfer duration remain unvaried. A greater thrust can considerably reduce the duration, "paying" this gain in ΔV and m_p: however, this can be convenient since by adding only $0{,}4\ Kg$ of fuel we can save more than a week in time duration. On the other hand, by doubling the initial mass, the fuel needed to perform the manoeuvre will increase as well as the global duration of it.

Conclusions

The major idea of this work is to offer private companies the subsystem required to maintain their payload in orbit for a variable lapse of time; thus, they will only need to support the cost of the payload's launch to the ISS – which could potentially be divided among different companies sharing the same launch – the cost of the transfer between the ISS and these platforms and the one associated with the required platform usage time. The first cost is already known, although it will probably and rapidly change in the next years, whereas the third one will depend of the platform itself. Thus, with this work, private companies will have an overview of the cost of the transfer and will be able to predict the cost of their entire mission. Maybe, one day, this project will be considered and, hopefully, this work will be used at starting point of it.